PASSIVE SENSOR IMAGING USING CROSS CORRELATIONS OF NOISY SIGNALS IN A SCATTERING MEDIUM

JOSSELIN GARNIER[*]AND GEORGE PAPANICOLAOU[†]

Abstract. It is well known that the travel time or even the full Green's function between two passive sensors can be estimated from the cross correlation of recorded signal amplitudes generated by ambient noise sources. It is also known that the direction of the energy flux from the noise sources affects the estimation of the travel time. Using the stationary phase method we show here that the travel time can be effectively estimated when the ray joining the two sensors continues into the noise source region. We extend this analysis to passive sensor imaging of reflectors with different ambient noise source configurations by suitably migrating the cross correlations. If in addition there is multiple scattering in the medium then reflectors can be imaged with passive sensor networks or arrays by migrating suitable fourth-order cross correlations. Fourth-order cross correlations can also be used with auxiliary passive sensors in order to enhance travel time estimation in a scattering medium.

Key words. Travel time estimation, passive sensor imaging, noise sources, random media.

AMS subject classifications. 35R30, 35R60, 86A15, 78A46

1. Introduction. The travel time between two sensors in an inhomogeneous medium can be estimated using the coherent signals emitted by an impulse point source and recorded by them. It can also be estimated using the ambient incoherent noise by computing the cross correlation of noisy signals recorded by the sensors. The ambient noise is generated by sources that are randomly distributed in space and are statistically stationary in time. The cross correlation of signal amplitudes contains information about the Green's function of the wave equation from which the travel time can be obtained. The background propagation velocity can then be estimated from the travel times between sensors in a network covering the region of interest.

The first application of this technique was carried out in seismology where the sensors were seismic stations recording velocity fluctuations, the noise sources came from the nonlinear interaction of the ocean swell with the coast that generates surface waves [34], and the goal was to obtain an estimate of the background surface wave velocity map of a large part of the Earth. The idea of exploiting the ambient noise and using the cross correlation of noisy signals to retrieve information about travel times was first proposed in helioseismology and seismology [18, 24, 31]. It has been applied to background velocity estimation from regional to local scales [21, 32, 20], volcano monitoring [29, 12, 11], and petroleum prospecting [17]. In randomly layered media, correlation methods for imaging are analyzed in [19]. When the support of the random noise sources extends over all space and they are uncorrelated, that is, their spatial correlation is a delta function, it has been shown that the derivative of the cross correlation of the recorded signals is the symmetrized Green's function between the sensors [26]. This is also true with spatially localized noise source distributions provided the waves propagate within an ergodic cavity [15, 16, 2]. At the physical level this result can be obtained in both open and closed environments provided that the recorded signals are equipartitioned [22, 37, 25, 33, 23]. In an open environment this means that the recorded signals are an uncorrelated and isotropic superposition of

plane waves of all directions. In a closed environment it means that the recorded signals are superpositions of normal modes with random amplitudes that are statistically uncorrelated and identically distributed.

In many applications, however, the noise source distribution is spatially limited and the recorded signals are not equipartitioned. As a result, the waves recorded by the sensors are dominated by the flux coming from the direction of the noise sources. The cross correlations of the recorded signals depend on the orientation of these sensors relative to the direction of the energy flux. This affects significantly the quality of the estimate for the Green's function. It is good when the line between the sensors is along the direction of the energy flux and bad when it is perpendicular to it [34].

In this paper, in Sections 2-4 we present a brief review of travel time estimation and passive imaging of reflectors by cross correlation of signals emitted by ambient noise sources. We do with using the stationary phase method. The main contribution of the paper is the introduction of a self-consistent theoretical framework for the analysis of noise cross correlation based interferometric imaging techniques (Sections 5-8), which extend the coherent interferometric (CINT) imaging techniques [8, 9] that can deal with scattering media (Subsection 7.2). We also give an analytical justification of the coda fourth-order correlation technique proposed by Campillo and Stehly [13] for travel time estimation (Section 8). A more detailed description of Sections 5-8 is given below.

We use the stationary phase method to analyze the estimation of the travel time between two sensors from the cross correlation of recorded noisy signals. This asymptotic approach is valid when the decoherence time of the noise sources is small compared to the travel time between the two sensors. With this formulation we can analyze systematically the dependence of the estimate of the travel time on the orientation of the ray between the sensors to the direction of the energy flux from the noise sources.

We extend the stationary phase analysis to passive sensor imaging of reflectors with different noise source configurations. In the presence of reflectors, the cross correlations between any two sensors have, in addition to the main peaks at the travel times between them, other peaks at lag times related to travel times from the sensors to the reflectors. We analyze in detail the relation between the secondary peaks in the cross correlations and travel times between sensors and reflectors for different spatial noise source distributions. With this information we show how to image the reflectors by migrating truncated correlations. If we have sensor data both with and without the reflectors then we can migrate differences of the cross correlations. The resolution of the images depends in an essential way on the support of the ambient noise source distribution relative to both the locations of the sensors and the reflectors. These results are obtained in a medium with a deterministic, smoothly varying background.

If there is multiple scattering in the medium, as in a randomly inhomogeneous medium, reflectors can still be imaged with passive sensor networks or arrays by migrating suitable fourth-order cross correlations. In addition to the primary peak at the travel time between the sensors and the secondary peaks at the travel times between sensors and reflectors, the cross correlation function has a long oscillatory tail, a coda, due to the multiple scattering. This coda is difficult to distinguish from the fluctuations in the correlation due to the noise sources. Following the coherent interferometric (CINT) imaging ideas developed for broadband deterministic pulses in [8], we form space-time local cross correlations of the cross correlations and migrate

them. The space-time windows over which these local fourth-order cross correlations are computed is determined adaptively as described in [8].

Using the stationary phase method we also show that the travel time between two sensors can be estimated even in some unfavorable situations provided that special fourth-order correlation functions with auxiliary sensors are used. By unfavorable we mean that the main component of the energy flux from the noise sources is roughly perpendicular to the ray connecting the two sensors. It is essential that there is scattering in the medium in order that the fourth-order correlations can be used effectively for enhancing travel time estimation between the two sensors. This result explains analytically how the iterated cross correlation technique proposed by Campillo and Stehly [13] works.

The paper is organized as follows. In Sections 2-3 we present the approach to travel time estimation and imaging using cross correlations of noisy signals. In Sections 4-5 we analyze in detail the cross correlation technique. We study the relation between the cross correlation and the Green's function in Section 4. In Section 5 we use the stationary phase method to analyze the estimation of the travel time from the cross correlation function. In Section 6 we show how this technique can be used for imaging reflectors using only passive sensors. We show how iterated cross correlations can be used for imaging in a scattering medium in Section 7, and for travel time estimation in Section 8.

2. Random sources, random scattering and wave cross correlations. The wave fields that are recorded by various sensors and are then cross correlated have properties that are inherited from the nature of the sources that generate them as well as from the environment in which they propagate. Analytically the simplest case is that of wave fields due to random sources in a homogeneous medium, which we discuss in the next subsection. We then discuss wave field cross correlations in strongly and weakly scattering media in Subsection 2.2.

2.1. Wave cross correlations in a homogeneous medium with random sources. Let $u(t, \mathbf{x}_1)$ and $u(t, \mathbf{x}_2)$ denote the time-dependent wave fields recorded by two sensors at $\mathbf{x}_1$ and $\mathbf{x}_2$. Their cross correlation function over the time interval $[0, T]$ with time lag τ is given by

$$C_T(\tau, \mathbf{x}_1, \mathbf{x}_2) = \frac{1}{T} \int_0^T u(t, \mathbf{x}_1) u(t + \tau, \mathbf{x}_2) dt \,. \tag{2.1}$$

In a homogeneous medium, if the source of the waves is a space-time stationary random field that is also delta correlated in space and time, it has been shown [33, 26] that

$$\frac{\partial}{\partial \tau} C_T(\tau, \mathbf{x}_1, \mathbf{x}_2) \simeq -\left[G(\tau, \mathbf{x}_1, \mathbf{x}_2) - G(-\tau, \mathbf{x}_1, \mathbf{x}_2) \right], \tag{2.2}$$

where G is the Green's function. This approximate equality holds for T sufficiently large and provided some limiting absorption is introduced to regularize the integral. It is briefly analyzed mathematically in Subsection 4.3. The main point here is that the time-symmetrized Green's function can be obtained from the cross correlation if there is enough source diversity. In this case the wave field at any sensor is equipartitioned, in the sense that it is a superposition of uncorrelated plane waves of all directions. We can recover in particular the travel time $\tau(\mathbf{x}_1, \mathbf{x}_2)$ from the singular support of the cross correlation.
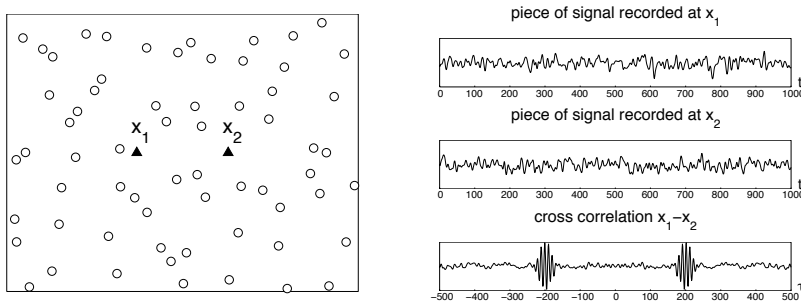
FIG. 2.1. *When the spatial support of the noise sources (circles) extends over all space then the cross correlation function is symmetric. The positive and negative parts correspond to the Green's function between $\mathbf{x}_1$ and $\mathbf{x}_2$ and its anti-causal counterpart, respectively.*

The configuration (Figure 2.1) in which the spatial support of the noise sources extends over all space is rarely encountered in practice. Significant departures from this ideal situation occur when limited spatial diversity of the sources introduces directivity into the recorded fields, which affects the quality of the estimate of the Green's function. If, in particular, the source distribution is spatially localized, then the flux of wave energy is not isotropic, and the cross correlation function is not symmetric (Figure 2.2). In some situations it may be impossible to distinguish the coherent part of the cross correlation function, which contains information about the travel time (Figure 2.3). A mathematical analysis is given in Section 5 using the stationary phase method.

2.2. Wave cross correlations in a scattering medium. In the case of a spatially localized distribution of noise sources, directional diversity of the recorded fields can be enhanced if there is sufficient scattering in the medium. An ergodic cavity with a homogeneous interior is a good example (Figure 2.4, left): Even with a source distribution that has very limited spatial support, the reverberations of the waves in the cavity generate interior fields with high directional diversity [15, 2]. Multiple scattering of waves by random inhomogeneities can also lead to wave field equipartition if the transport mean free path is short compared to the distance from the sources to the sensors [30, 21, 27]. The transport mean free path is the propagation distance over which wave energy transport in a scattering medium is effectively isotropic. In such a scattering medium (Figure 2.4, right), the inhomogeneities can be viewed as secondary sources in the vicinity of the sensors.

If in a random medium the transport mean free path is short compared to the distance between the sensors, then the cross correlation function still gives an estimate of the Green's function, which is itself random because of the medium. However, its coherent part that has information about the travel time is essentially unobservable. The travel time can be estimated in a random medium when the noise sources are spatially limited provided that (i) the transport mean free path is short compared to the distance between the sources and the sensors, and (ii) it is long compared to the distance between the sensors.

3. Background velocity estimation and imaging. In this section we consider the two main reasons for estimating travel times from cross correlations. The first one, to which most of the recent work in geophysics is devoted, concerns background
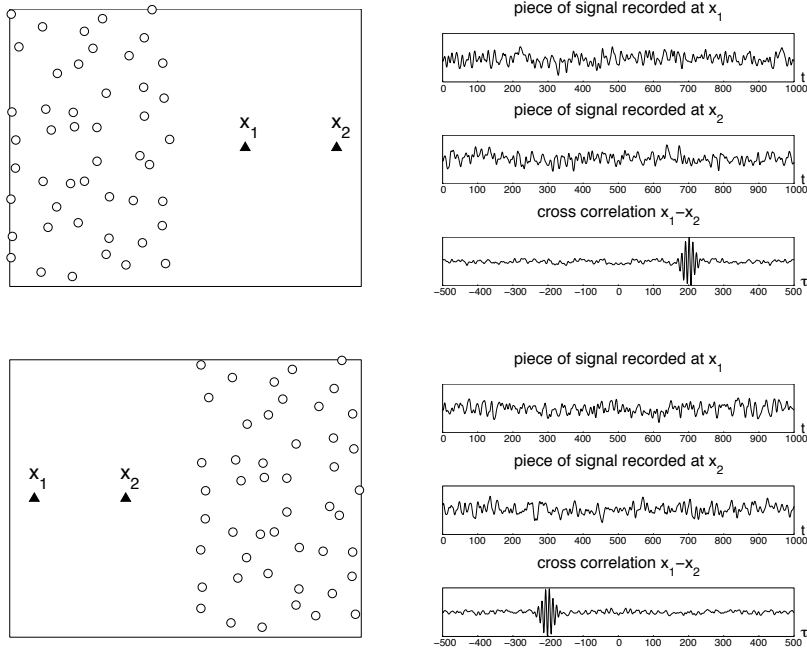
FIG. 2.2. *When the distribution of noise sources is spatially localized then the cross correlation function is not symmetric.*
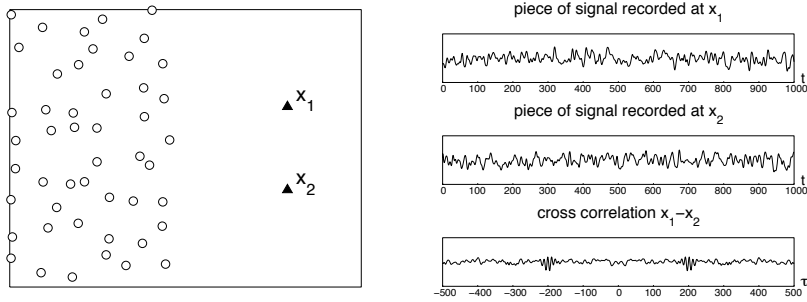

FIG. 2.3. *When the distribution of noise sources is spatially localized then the coherent part of the cross correlation function can be difficult or even impossible to distinguish if the axis formed by the two sensors is perpendicular to the main direction of energy flux from the noise sources.*

velocity estimation and is presented in Subsection 3.1. The second one concerns imaging of reflectors using passive sensor networks and arrays. This is presented in Subsection 3.2. In Subsection 3.3 we discuss how iterated cross correlation techniques can be used in scattering media both for imaging and background velocity estimation.

3.1. Background velocity estimation. From the travel times between sensors in a network we can estimate tomographically the background propagation velocity [3]. In seismic imaging, velocity estimation is usually done by other methods [35, 4]. It is clear that the density and topology of the sensor network, as well as the quality
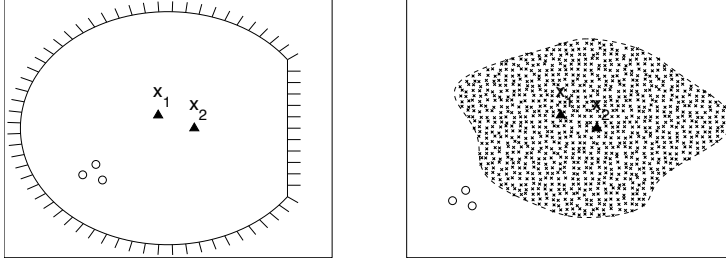
FIG. 2.4. *Configurations in which wave fields have directional diversity. An ergodic cavity (left figure) and a randomly inhomogeneous medium (right figure).*

of the travel times estimates, influence the spatial resolution and the accuracy of the reconstructed velocity map. Tomographic travel time velocity analysis using dispersion curves of surface waves derived from noise correlations was applied successfully in Southern California [28], in Tibet [38], and in the Alps [34].

3.2. Array and distributed passive sensor imaging. The main purpose of this paper is to show that travel time estimation using cross correlations can also be used for passive sensor imaging. Consider an array of passive sensors located at $(\mathbf{x}_j)_{j=1,\ldots,N}$, which record signals emitted by random sources, and point reflectors located at $(\mathbf{z}_{\mathrm{r},j})_{j=1,\ldots,N_r}$. The recorded signals are denoted $u(t,\mathbf{x}_j)$, $j=1,\ldots,N$. In imaging we want to estimate the locations of the reflectors from this data set. If the impulse response matrix $P(\mathbf{x}_j,\mathbf{x}_l,t)$ of the sensor network is known, even partially, then the usual migration techniques [4, 14] that back propagate the impulse responses numerically in a fictitious medium give estimates of the locations of the reflectors. Knowing the impulse response matrix requires, however, an active, broadband sensor network. This is because each sensor must emit an impulse that propagates in the medium and its echoes are then recorded by all the sensors. In Section 6 we show how the impulse response matrix of a sensor network with passive sensors can be estimated from the matrix of cross correlations

$$C_T(\tau,\mathbf{x}_j,\mathbf{x}_l) = \frac{1}{T}\int_0^T u(t,\mathbf{x}_j)u(t+\tau,\mathbf{x}_l)dt\,, \quad j,l = 1,\ldots,N\,. \qquad (3.1)$$

In the presence of reflectors, the structure of the cross correlation between two sensors is more complex because it has additional peaks at arrival times between the sensors and the reflectors. These peaks are, however, relatively weak. In order that they can be effective in migration imaging we must either mask the main peaks at the travel times between the sensors, or subtract them if we have available sensor cross correlations in the absence of the reflectors.

Background velocity estimation is a preliminary step in implementing travel time migration, which is done numerically in a background medium with the estimated velocity. It is important to have some knowledge of the background velocity of the medium so that the numerical back propagation of the cross correlations will focus with good resolution near the correct reflector locations.

3.3. Interferometric travel time estimation and imaging in scattering media with iterated cross correlations. Another contribution presented here, in

Section 7, is the use of iterated cross correlations to image reflectors in a scattering medium. By a scattering medium we mean a large collection of small random scatterers which we do not want to image, but which generate multiply scattered waves. As a result, the structure of the Green's functions and, therefore, that of the cross correlations is more complex. In addition to the singular components corresponding to the arrival of the direct waves and of the waves interacting with the reflectors, which we want to image, the Green's functions and the cross correlations have long incoherent tails, or coda, that come from the multiply scattered waves.

When migrating these cross correlations numerically using the estimated background velocity, the resulting images are distorted and have a lot of speckles. The reason for this is that the coda due to the multiple scattering is also migrated. It is not possible to remove the coda from the cross correlations because the singular components due to the reflectors are buried in it. A natural way to reduce the adverse effects of multiple scattering is to use iterated cross correlations, after removing the principal singular components corresponding to the arrival times between the sensors. In order to be effective, the calculation of the iterated cross correlations must be done over adaptively estimated space-time windows as is done in coherent interferometric (CINT) imaging [8]. Adaptive CINT was introduced for active array and distributed sensor imaging in a scattering medium when the impulse response matrix is known. In Section 7 we describe how CINT can be used for passive array imaging in a scattering medium.

Multiple scattering can be advantageous in estimating the travel time between sensors because it enhances the directional diversity of the wave fields. The enhanced diversity is, however, in the incoherent coda of the cross correlations. In order to exploit it we can use iterated cross correlations with auxiliary sensors as suggested by Campillo and Stehly [13]. This iterated cross correlation technique is analyzed in Section 8 using the stationary phase method.

4. Extracting the Green's function from the cross correlation.

4.1. The wave equation with noise sources. We consider the solution u of the wave equation in a d-dimensional inhomogeneous medium:

$$\frac{1}{c^2(\mathbf{x})} \frac{\partial^2 u}{\partial t^2} - \Delta_{\mathbf{x}} u = n^\varepsilon(t, \mathbf{x}). \tag{4.1}$$

The term $n^\varepsilon(t, \mathbf{x})$ models a random distribution of noise sources. It is a zero-mean stationary (in time) Gaussian process with autocorrelation function

$$\langle n^\varepsilon(t_1, \mathbf{y}_1) n^\varepsilon(t_2, \mathbf{y}_2) \rangle = F^\varepsilon(t_2 - t_1) \Gamma(\mathbf{y}_1, \mathbf{y}_2). \tag{4.2}$$

Here $\langle \cdot \rangle$ stands for statistical average with respect to the distribution of the noise sources. The Gaussian property is assumed here so as to simplify the calculations of statistical stability in Appendix A. It could be replaced by a more general decorrelation or mixing property. We assume that the decoherence time of the noise sources is much smaller than typical travel times between sensors. If we denote with ε the (small) ratio of these two time scales, we can then write the time correlation function F^ε in the form

$$F^\varepsilon(t_2 - t_1) = F\left(\frac{t_2 - t_1}{\varepsilon}\right), \tag{4.3}$$

where t_1 and t_2 are scaled relative to typical sensor travel times. The Fourier transform $\hat{F}^\varepsilon$ of the time correlation function is a nonnegative, even real-valued function. It is

proportional to the power spectral density of the sources:

$$\hat{F}^\varepsilon(\omega) = \varepsilon \hat{F}(\varepsilon\omega)\,, \tag{4.4}$$

where the Fourier transform is defined by

$$\hat{F}(\omega) = \int F(t) e^{i\omega t}\, dt\,. \tag{4.5}$$

The spatial distribution of the noise sources is characterized by the auto-covariance function Γ. It is the kernel of a symmetric nonnegative definite operator. For simplicity, we will assume that the process n^ε is delta-correlated in space:

$$\Gamma(\mathbf{y}_1, \mathbf{y}_2) = \theta(\mathbf{y}_1)\delta(\mathbf{y}_1 - \mathbf{y}_2)\,, \tag{4.6}$$

where θ characterizes the spatial support of the sources. It is possible to consider a more general form for the spatial auto-covariance function, as in [2], but this complicates the calculations without changing the results qualitatively.

4.2. Statistical stability of the cross correlation function. The stationary solution of the wave equation has the integral representation

$$u(t, \mathbf{x}) = \int\int_{-\infty}^{t} n^\varepsilon(s, \mathbf{y}) G(t - s, \mathbf{x}, \mathbf{y})\, ds\, d\mathbf{y}$$
$$= \int\int n^\varepsilon(t - s, \mathbf{y}) G(s, \mathbf{x}, \mathbf{y})\, ds\, d\mathbf{y}\,, \tag{4.7}$$

where $G(t, \mathbf{x}, \mathbf{y})$ is the time-dependent Green's function. It is the fundamental solution of the wave equation

$$\frac{1}{c^2(\mathbf{x})}\frac{\partial^2 G}{\partial t^2} - \Delta_\mathbf{x} G = \delta(t)\delta(\mathbf{x} - \mathbf{y})\,, \tag{4.8}$$

starting from $G(0, \mathbf{x}, \mathbf{y}) = \partial_t G(0, \mathbf{x}, \mathbf{y}) = 0$ (and continued on the negative time axis by $G(t, \mathbf{x}, \mathbf{y}) = 0 \ \forall t \le 0$).

The empirical cross correlation of the signals recorded at $\mathbf{x}_1$ and $\mathbf{x}_2$ for an integration time T is

$$C_T(\tau, \mathbf{x}_1, \mathbf{x}_2) = \frac{1}{T}\int_0^T u(t, \mathbf{x}_1) u(t + \tau, \mathbf{x}_2)\, dt\,. \tag{4.9}$$

It is a statistically stable quantity, in the sense that for a large integration time T, C_T is independent of the realization of the noise sources. This is stated in the following proposition proved in Appendix A.

PROPOSITION 4.1. *1. The expectation of C_T (with respect to the distribution of the sources) is independent of T:*

$$\langle C_T(\tau, \mathbf{x}_1, \mathbf{x}_2)\rangle = C^{(1)}(\tau, \mathbf{x}_1, \mathbf{x}_2)\,, \tag{4.10}$$

where $C^{(1)}$ is given by

$$C^{(1)}(\tau, \mathbf{x}_1, \mathbf{x}_2) = \int d\mathbf{y}\int ds\, ds'\, G(s, \mathbf{x}_1, \mathbf{y}) G(\tau + s + s', \mathbf{x}_2, \mathbf{y}) F^\varepsilon(s')\theta(\mathbf{y})\,, \tag{4.11}$$

or equivalently by

$$C^{(1)}(\tau, \mathbf{x}_1, \mathbf{x}_2) = \frac{1}{2\pi} \int d\mathbf{y} \int d\omega \overline{\hat{G}(\omega, \mathbf{x}_1, \mathbf{y})} \hat{G}(\omega, \mathbf{x}_2, \mathbf{y}) \hat{F}^\varepsilon(\omega) e^{-i\omega\tau} \theta(\mathbf{y}). \qquad (4.12)$$

2. The empirical cross correlation C_T is a self-averaging quantity:

$$C_T(\tau, \mathbf{x}_1, \mathbf{x}_2) \overset{T \to \infty}{\longrightarrow} C^{(1)}(\tau, \mathbf{x}_1, \mathbf{x}_2), \qquad (4.13)$$

in probability with respect to the distribution of the sources. More precisely, the fluctuations of C_T around its mean value $C^{(1)}$ are of order $T^{-1/2}$ for T large compared to the decoherence time of the sources. The asymptotic covariance function of C_T is given by (A.4).

Both expressions (4.11) and (4.12) will be used in the following sections.

4.3. Emergence of the Green's function for an extended distribution of sources in a homogeneous medium. We give an elementary proof of the relation between the cross correlation and the Green's function when the medium is homogeneous with background velocity c_0 and the source distribution extends over all space, i.e. $\theta \equiv 1$, as in Figure 2.1. In this case the signal amplitude diverges because the contributions from noise sources far away from the sensors are not damped. For a well-posed formulation we need to introduce some dissipation, so we consider the solution u of the damped wave equation:

$$\frac{1}{c_0^2}\left(\frac{1}{T_a} + \frac{\partial}{\partial t}\right)^2 u - \Delta_{\mathbf{x}} u = n^\varepsilon(t, \mathbf{x}). \qquad (4.14)$$

A somewhat different form of the following proposition, with delta-correlated in time sources and with a different definition of dissipation, can be found in [26].

PROPOSITION 4.2. *In a three-dimensional open medium with dissipation and if the source distribution extends over all space, so that $\theta \equiv 1$, then*

$$\frac{\partial}{\partial\tau}C^{(1)}(\tau, \mathbf{x}_1, \mathbf{x}_2) = -\frac{c_0^2 T_a}{4} e^{-\frac{|\mathbf{x}_1-\mathbf{x}_2|}{c_0 T_a}} \left[F^\varepsilon * G(\tau, \mathbf{x}_1, \mathbf{x}_2) - F^\varepsilon * G(-\tau, \mathbf{x}_1, \mathbf{x}_2)\right], \quad (4.15)$$

where $*$ stands for the convolution in τ and G is the Green's function of the homogeneous medium without dissipation:

$$G(t, \mathbf{x}_1, \mathbf{x}_2) = \frac{1}{4\pi|\mathbf{x}_1 - \mathbf{x}_2|} \delta\left(t - \frac{|\mathbf{x}_1 - \mathbf{x}_2|}{c_0}\right).$$

If the decoherence time of the sources is much shorter than the travel time (i.e., $\varepsilon \ll 1$), then F^ε behaves like a Dirac distribution in (4.15) and we have

$$\frac{\partial}{\partial\tau}C^{(1)}(\tau, \mathbf{x}_1, \mathbf{x}_2) \simeq -e^{-\frac{|\mathbf{x}_1-\mathbf{x}_2|}{c_0 T_a}} \left[G(\tau, \mathbf{x}_1, \mathbf{x}_2) - G(-\tau, \mathbf{x}_1, \mathbf{x}_2)\right],$$

up to a multiplicative constant. It is therefore possible to estimate the travel time $\tau(\mathbf{x}_1, \mathbf{x}_2) = |\mathbf{x}_1 - \mathbf{x}_2|/c_0$ between $\mathbf{x}_1$ and $\mathbf{x}_2$ from the cross correlation, with an accuracy of the order of the decoherence time of the noise sources.

Proof. The Green's function of the homogeneous medium with dissipation is:

$$G_a(t, \mathbf{x}_1, \mathbf{x}_2) = G(t, \mathbf{x}_1, \mathbf{x}_2) e^{-\frac{t}{T_a}}.$$

The cross correlation function is given by (4.11):

$$C^{(1)}(\tau, \mathbf{x}_1, \mathbf{x}_2) = \int d\mathbf{y} \int ds ds' G_a(s, \mathbf{x}_1, \mathbf{y}) G_a(\tau + s + s', \mathbf{x}_2, \mathbf{y}) F^\varepsilon(s').$$

Integrating in s and s' gives

$$C^{(1)}(\tau, \mathbf{x}_1, \mathbf{x}_2) = \int \frac{d\mathbf{y}}{16\pi^2 |\mathbf{x}_1 - \mathbf{y}| \, |\mathbf{x}_2 - \mathbf{y}|} e^{-\frac{|\mathbf{x}_1 - \mathbf{y}| + |\mathbf{x}_2 - \mathbf{y}|}{c_0 T_a}} F^\varepsilon\left(\tau - \frac{|\mathbf{x}_1 - \mathbf{y}| - |\mathbf{x}_2 - \mathbf{y}|}{c_0}\right).$$

We parameterize the locations of the sensors by $\mathbf{x}_1 = (h, 0, 0)$ and $\mathbf{x}_2 = (-h, 0, 0)$, where $h > 0$, and we use the change of variables for $\mathbf{y} = (x, y, z)$:

$$\begin{cases} x = h \sin \eta \cosh \phi, & \phi \in (0, \infty), \\ y = h \cos \eta \sinh \phi \cos \psi, & \eta \in (-\pi/2, \pi/2), \\ z = h \cos \eta \sinh \phi \sin \psi, & \psi \in (0, 2\pi), \end{cases}$$

whose Jacobian is $J = h^3 \cos \eta \sinh \phi (\cosh^2 \phi - \sin^2 \eta)$. Using the fact that $|\mathbf{x}_1 - \mathbf{y}| = h(\cosh \phi - \sin \eta)$ and $|\mathbf{x}_2 - \mathbf{y}| = h(\cosh \phi + \sin \eta)$, we get

$$C^{(1)}(\tau, \mathbf{x}_1, \mathbf{x}_2) = \frac{h}{8\pi} \int_0^\infty d\phi \sinh \phi \int_{-\pi/2}^{\pi/2} d\eta \cos \eta \, e^{-\frac{2h \cosh \phi}{c_0 T_a}} F^\varepsilon\left(\tau + \frac{2h \sin \eta}{c_0}\right).$$

After the new change of variables $u = h \cosh \phi$ and $s = (2h/c_0) \sin \eta$, we obtain

$$C^{(1)}(\tau, \mathbf{x}_1, \mathbf{x}_2) = \frac{c_0^2 T_a}{32\pi h} e^{-\frac{2h}{c_0 T_a}} \int_{-2h/c_0}^{2h/c_0} F^\varepsilon(\tau + s) ds.$$

By differentiating in τ, we get

$$\frac{\partial}{\partial \tau} C^{(1)}(\tau, \mathbf{x}_1, \mathbf{x}_2) = \frac{c_0^2 T_a}{32\pi h} e^{-\frac{2h}{c_0 T_a}} \left[F^\varepsilon\left(\tau + \frac{2h}{c_0}\right) - F^\varepsilon\left(\tau - \frac{2h}{c_0}\right) \right],$$

which is the desired result since $|\mathbf{x}_1 - \mathbf{x}_2| = 2h$. $\qquad\square$

4.4. Emergence of the Green's function for an extended distribution of sources in an inhomogeneous medium. The cross correlation function is closely related to the symmetrized Green's function from $\mathbf{x}_1$ to $\mathbf{x}_2$ not only for a homogeneous medium but also for inhomogeneous media, as discussed in the introduction. Here we give a simple and rigorous proof for an open inhomogeneous medium in the case in which the noise sources are located on the surface of a sphere that encloses both the inhomogeneous region and the sensors, located at $\mathbf{x}_1$ and $\mathbf{x}_2$. The proof is based on an approximate identity that follows from Green's identity and the Sommerfeld radiation condition. This approximate identity can be viewed as a version of the Helmholtz-Kirchhoff integral theorem (known in acoustics [5, p. 473] and in optics [10, p. 419]) and it is also presented in [36].

PROPOSITION 4.3. *Let us assume that the medium is homogeneous with background velocity c_e outside the ball $B(\mathbf{0}, D)$ with center $\mathbf{0}$ and radius D. Then, for any $\mathbf{x}_1, \mathbf{x}_2 \in B(\mathbf{0}, D)$ we have for $L \gg D$:*

$$\hat{G}(\omega, \mathbf{x}_1, \mathbf{x}_2) - \overline{\hat{G}}(\omega, \mathbf{x}_1, \mathbf{x}_2) = \frac{2i\omega}{c_e} \int_{\partial B(\mathbf{0}, L)} \overline{\hat{G}}(\omega, \mathbf{x}_1, \mathbf{y}) \hat{G}(\omega, \mathbf{x}_2, \mathbf{y}) d\sigma(\mathbf{y}). \qquad (4.16)$$

Proof. We consider the equation satisfied by the time-harmonic Green's function with the source at $\mathbf{x}_2$ and the complex conjugate form of this equation with the source at $\mathbf{x}_1$:

$$\Delta_{\mathbf{y}}\hat{G}(\omega,\mathbf{y},\mathbf{x}_2) + \frac{\omega^2}{c^2(\mathbf{y})}\hat{G}(\omega,\mathbf{y},\mathbf{x}_2) = -\delta(\mathbf{y}-\mathbf{x}_2)\,,$$

$$\Delta_{\mathbf{y}}\overline{\hat{G}}(\omega,\mathbf{y},\mathbf{x}_1) + \frac{\omega^2}{c^2(\mathbf{y})}\overline{\hat{G}}(\omega,\mathbf{y},\mathbf{x}_1) = -\delta(\mathbf{y}-\mathbf{x}_1)\,.$$

We multiply the first equation by $\overline{\hat{G}}(\omega,\mathbf{y},\mathbf{x}_1)$ and subtract the second equation multiplied by $\hat{G}(\omega,\mathbf{y},\mathbf{x}_2)$:

$$\nabla_{\mathbf{y}}\cdot\left[\overline{\hat{G}}(\omega,\mathbf{y},\mathbf{x}_1)\nabla_{\mathbf{y}}\hat{G}(\omega,\mathbf{y},\mathbf{x}_2) - \hat{G}(\omega,\mathbf{y},\mathbf{x}_2)\nabla_{\mathbf{y}}\overline{\hat{G}}(\omega,\mathbf{y},\mathbf{x}_1)\right]$$

$$= \hat{G}(\omega,\mathbf{y},\mathbf{x}_2)\delta(\mathbf{y}-\mathbf{x}_1) - \overline{\hat{G}}(\omega,\mathbf{y},\mathbf{x}_1)\delta(\mathbf{y}-\mathbf{x}_2)$$

$$= \hat{G}(\omega,\mathbf{x}_1,\mathbf{x}_2)\delta(\mathbf{y}-\mathbf{x}_1) - \overline{\hat{G}}(\omega,\mathbf{x}_1,\mathbf{x}_2)\delta(\mathbf{y}-\mathbf{x}_2)\,,$$

where we have used the reciprocity property $\hat{G}(\omega,\mathbf{x}_2,\mathbf{x}_1) = \hat{G}(\omega,\mathbf{x}_1,\mathbf{x}_2)$. We next integrate over the ball $B(\mathbf{0},L)$ and use the divergence theorem:

$$\int_{\partial B(\mathbf{0},L)}\mathbf{n}\cdot\left[\overline{\hat{G}}(\omega,\mathbf{y},\mathbf{x}_1)\nabla_{\mathbf{y}}\hat{G}(\omega,\mathbf{y},\mathbf{x}_2) - \hat{G}(\omega,\mathbf{y},\mathbf{x}_2)\nabla_{\mathbf{y}}\overline{\hat{G}}(\omega,\mathbf{y},\mathbf{x}_1)\right]d\sigma(\mathbf{y})$$

$$= \hat{G}(\omega,\mathbf{x}_1,\mathbf{x}_2) - \overline{\hat{G}}(\omega,\mathbf{x}_1,\mathbf{x}_2)\,,$$

where $\mathbf{n}$ is the unit outward normal to the ball $B(\mathbf{0},L)$, which is $\mathbf{n}=\mathbf{y}/|\mathbf{y}|$. This equality can be viewed as an application of the Green's second identity. The Green's function also satisfies the Sommerfeld radiation condition

$$\lim_{|\mathbf{y}|\to\infty}|\mathbf{y}|^{\frac{d-1}{2}}\left(\frac{\mathbf{y}}{|\mathbf{y}|}\cdot\nabla_{\mathbf{y}} - i\frac{\omega}{c_e}\right)\hat{G}(\omega,\mathbf{y},\mathbf{x}_1) = 0\,,$$

uniformly in all directions $\mathbf{y}/|\mathbf{y}|$. Under the conditions stated in the proposition, we can substitute $i(\omega/c_e)\hat{G}(\omega,\mathbf{y},\mathbf{x}_2)$ for $\mathbf{n}\cdot\nabla_{\mathbf{y}}\hat{G}(\omega,\mathbf{y},\mathbf{x}_2)$ in the surface integral over $\partial B(\mathbf{0},L)$, and $-i(\omega/c_e)\overline{\hat{G}}(\omega,\mathbf{y},\mathbf{x}_1)$ for $\mathbf{n}\cdot\nabla_{\mathbf{y}}\overline{\hat{G}}(\omega,\mathbf{y},\mathbf{x}_1)$, which gives the desired result.

Note that it is important that the medium be homogeneous in the exterior of the ball $B(\mathbf{0},D)$ in order be able to use the radiation condition. □

The right side of the Helmholtz-Kirchhoff identity (4.16) is related to the representation (4.12) of the cross correlation function $C^{(1)}$ in the Fourier domain. Therefore, by substituting (4.16) into (4.12) we get the following corollary.

COROLLARY 4.4. *We assume that*
1) the medium is homogeneous with background velocity c_e outside the ball $B(\mathbf{0},D)$ with center $\mathbf{0}$ and radius D,
2) the sources are localized with a uniform density on the sphere $\partial B(\mathbf{0},L)$ with center $\mathbf{0}$ and radius L.
If $L \gg D$, then for any $\mathbf{x}_1, \mathbf{x}_2 \in B(\mathbf{0},D)$

$$\frac{\partial}{\partial\tau}C^{(1)}(\tau,\mathbf{x}_1,\mathbf{x}_2) \simeq -\left[F^{\varepsilon}*G(\tau,\mathbf{x}_1,\mathbf{x}_2) - F^{\varepsilon}*G(-\tau,\mathbf{x}_1,\mathbf{x}_2)\right],\qquad(4.17)$$

up to a multiplicative factor. Here $*$ stands for convolution in τ.

If in addition we have $\varepsilon \ll 1$, then F^ε behaves approximately like a delta distribution acting on the Green's function and we get the form (2.2).

In proving the identity (2.2) in the previous subsections it was necessary that the noise source distribution generate an isotropic field at the sensors, coming from all directions. In the next sections we will consider cases in which this isotropy condition is not fulfilled.

5. Stationary phase analysis for travel time estimation with spatially localized noise sources. We study in this section the cross correlation function when the support of the sources is spatially limited. We assume that the fluctuations of the medium parameters are modeled by a smooth background velocity profile $c_0(\mathbf{x})$ which is homogeneous outside a large sphere that encloses the sensors and the sources. The outgoing time-harmonic Green's function $\hat{G}_0$ of the medium is the solution of

$$\Delta_{\mathbf{x}} \hat{G}_0(\omega, \mathbf{x}, \mathbf{y}) + \frac{\omega^2}{c_0^2(\mathbf{x})} \hat{G}_0(\omega, \mathbf{x}, \mathbf{y}) = -\delta(\mathbf{x} - \mathbf{y}), \qquad (5.1)$$

along with the radiation condition at infinity. When the background is homogeneous with constant wave speed c_0 and wavenumber $k = \omega/c_0$, then the homogeneous outgoing time-harmonic Green's function is

$$\hat{G}_0(\omega, \mathbf{x}, \mathbf{y}) = \frac{e^{ik|\mathbf{y}-\mathbf{x}|}}{4\pi|\mathbf{y} - \mathbf{x}|} \qquad (5.2)$$

in three-dimensional space, and

$$\hat{G}_0(\omega, \mathbf{x}, \mathbf{y}) = \frac{i}{4} H_0^{(1)}(k|\mathbf{y} - \mathbf{x}|) \qquad (5.3)$$

in two-dimensional space. Here $H_0^{(1)}$ is the zeroth order Hankel function of the first kind. Because of our scaling assumptions regarding the form (4.4) of the power spectral density of the noise sources, we will have to evaluate the time-harmonic Green's function at frequencies of the form ω/ε. Using the asymptotic form of the Hankel function [1, formula 9.2.3], we see that the high-frequency behavior of the Green's function is related to the homogeneous medium travel time $|\mathbf{x} - \mathbf{y}|/c_0$:

$$\hat{G}_0\left(\frac{\omega}{\varepsilon}, \mathbf{x}, \mathbf{y}\right) \sim \frac{1}{|\mathbf{x} - \mathbf{y}|^{(d-1)/2}} e^{i\frac{\omega}{\varepsilon}\frac{|\mathbf{x}-\mathbf{y}|}{c_0}}.$$

For a general smoothly varying background with propagation speed $c_0(\mathbf{x})$, the high-frequency behavior of the Green's function is also related to the travel time and it is given by the WKB (Wentzel-Kramers-Brillouin) approximation [6]

$$\hat{G}_0\left(\frac{\omega}{\varepsilon}, \mathbf{x}, \mathbf{y}\right) \sim a(\mathbf{x}, \mathbf{y}) e^{i\frac{\omega}{\varepsilon}\tau(\mathbf{x},\mathbf{y})}, \qquad (5.4)$$

which is valid when $\varepsilon \ll 1$. Here the coefficients $a(\mathbf{x}, \mathbf{y})$ and $\tau(\mathbf{x}, \mathbf{y})$ are smooth except at $\mathbf{x} = \mathbf{y}$. The amplitude $a(\mathbf{x}, \mathbf{y})$ satisfies a transport equation and the travel time $\tau(\mathbf{x}, \mathbf{y})$ satisfies the eikonal equation. It is a symmetric function, $\tau(\mathbf{x}, \mathbf{y}) = \tau(\mathbf{y}, \mathbf{x})$, and it can be obtained from Fermat's principle

$$\tau(\mathbf{x}, \mathbf{y}) = \inf\left\{T \text{ s.t. } \exists (\mathbf{X}_t)_{t \in [0,T]} \in \mathcal{C}^1, \ \mathbf{X}_0 = \mathbf{x}, \ \mathbf{X}_T = \mathbf{y}, \ \left|\frac{d\mathbf{X}_t}{dt}\right| = c_0(\mathbf{X}_t)\right\}. \quad (5.5)$$
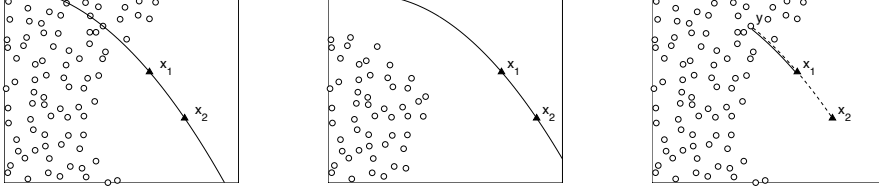
FIG. 5.1. *If the ray going through* $\mathbf{x}_1$ *and* $\mathbf{x}_2$ *(solid line) enters into the source region (left figure), then the travel time can be estimated from the cross correlation. If this is not the case, then the cross correlation does not have a peak at the travel time (middle figure). Right figure: The main contribution to the singular components of the cross correlation is from pairs of ray segments issuing from a source* $\mathbf{y}$ *going to* $\mathbf{x}_1$ *and to* $\mathbf{x}_2$, *respectively (solid and dashed lines, respectively), and starting in the same direction.*

A curve $(\mathbf{X}_t)_{t \in [0,T]}$ that produces the minimum in (5.5) is a ray and it satisfies Hamilton's equations (see Appendix B). For simplicity we assume that the background speed $c_0(\mathbf{x})$ is such that there is a unique ray joining any pair of points $(\mathbf{x}, \mathbf{y})$ in the region of interest.

We can now describe the behavior of the cross correlation function between $\mathbf{x}_1$ and $\mathbf{x}_2$ when ε is small, with and without directional energy flux from the sources.

PROPOSITION 5.1. *As* ε *tends to zero, the cross correlation* $C^{(1)}(\tau, \mathbf{x}_1, \mathbf{x}_2)$ *has singular components if and only if the ray going through* $\mathbf{x}_1$ *and* $\mathbf{x}_2$ *reaches into the source region, that is, into the support of the function* θ. *In this case there are either one or two singular components at* $\tau = \pm\tau(\mathbf{x}_1, \mathbf{x}_2)$.

More precisely, any ray going from the source region to $\mathbf{x}_2$ *and then to* $\mathbf{x}_1$ *gives rise to a singular component at* $\tau = -\tau(\mathbf{x}_1, \mathbf{x}_2)$. *Rays going from the source region to* $\mathbf{x}_1$ *and then to* $\mathbf{x}_2$ *give rise to a singular component at* $\tau = \tau(\mathbf{x}_1, \mathbf{x}_2)$.

This proposition explains why travel time estimation is bad when the ray joining $\mathbf{x}_1$ and $\mathbf{x}_2$ is roughly perpendicular to the direction of the energy flux from the noise sources, as in the middle of Figure 5.1.

The stationary phase contributions to the singular components of the cross correlation come from pairs of ray segments. The first ray goes from a source point to $\mathbf{x}_2$ and the second ray goes from the same source point and with the same initial angle to $\mathbf{x}_1$. The singular component is then concentrated at the difference of the travel times between these two ray segments. In the configuration on the right in Figure 5.1 the contribution to the singular component is at $\tau = \tau(\mathbf{x}_1, \mathbf{x}_2)$.

Proof. Using (4.12) we have

$$C^{(1)}(\tau, \mathbf{x}_1, \mathbf{x}_2) = \frac{1}{2\pi} \int d\mathbf{y} \int d\omega \overline{\hat{G}_0}\Big(\frac{\omega}{\varepsilon}, \mathbf{x}_1, \mathbf{y}\Big) \hat{G}_0\Big(\frac{\omega}{\varepsilon}, \mathbf{x}_2, \mathbf{y}\Big) e^{-i\frac{\omega}{\varepsilon}\tau} \hat{F}(\omega) \theta(\mathbf{y}) \,.$$

First we use the WKB approximation (5.4) of the Green's function and obtain

$$C^{(1)}(\tau, \mathbf{x}_1, \mathbf{x}_2) = \frac{1}{2\pi} \int d\mathbf{y}\theta(\mathbf{y}) \int d\omega \hat{F}(\omega) \overline{a}(\mathbf{x}_1, \mathbf{y}) a(\mathbf{x}_2, \mathbf{y}) e^{i\frac{\omega}{\varepsilon}\mathcal{T}(\mathbf{y})} \,,$$

where the rapid phase is

$$\omega\mathcal{T}(\mathbf{y}) = \omega[\tau(\mathbf{x}_2, \mathbf{y}) - \tau(\mathbf{x}_1, \mathbf{y}) - \tau] \,. \tag{5.6}$$

By the stationary phase method [6], the dominant contribution comes from the stationary points $(\omega, \mathbf{y})$ of the phase which satisfy

$$\partial_\omega \Big(\omega \mathcal{T}(\mathbf{y}) \Big) = 0 \,, \quad \nabla_\mathbf{y} \Big(\omega \mathcal{T}(\mathbf{y}) \Big) = \mathbf{0} \,.$$

This implies that

$$\tau(\mathbf{y}, \mathbf{x}_2) - \tau(\mathbf{y}, \mathbf{x}_1) = \tau \,, \quad \nabla_\mathbf{y} \tau(\mathbf{y}, \mathbf{x}_2) = \nabla_\mathbf{y} \tau(\mathbf{y}, \mathbf{x}_1) \,.$$

By Lemma B.1 in the appendix, the second condition requires that $\mathbf{x}_1$ and $\mathbf{x}_2$ lie on the same side of a ray issuing from a point $\mathbf{y}$. If the points are aligned along the ray as $\mathbf{y} \to \mathbf{x}_1 \to \mathbf{x}_2$, then the first condition is equivalent to $\tau = \tau(\mathbf{x}_1, \mathbf{x}_2)$. If the points are aligned along the ray as $\mathbf{y} \to \mathbf{x}_2 \to \mathbf{x}_1$, then the first condition is equivalent to $\tau = -\tau(\mathbf{x}_1, \mathbf{x}_2)$. The stationary points $\mathbf{y}$ contribute to the integral only if they are in the support of θ, which is the source region. This completes the proof of the proposition.   □

6. Passive sensor imaging with cross correlations. In this section we show using again the stationary phase method that it is possible to image reflectors by cross correlations of signal amplitudes generated by ambient noise sources and recorded by passive sensors. We assume here that the background medium is homogeneous or smoothly varying. Background media with random inhomogeneities and multiple scattering are considered in Section 7.

6.1. Identification of singular components of cross correlations for different configurations of sources sensors and reflectors. The stationary phase analysis in the following subsection indicates that we should distinguish three types of configurations of sources, sensors and reflectors (Figure 6.1). We use terminology from analogous situations in photography but it should be kept in mind that imaging is coherent here, which means that the recorded signals are time-resolved amplitudes and not just intensities.
1) The noise sources surround both the sensors and the reflectors. We call this the surround light configuration.
2) The noise sources are spatially localized and the sensors are between the sources and the reflectors. More precisely, these are configurations in which rays going through reflectors and sensors reach into the source region, and the sensors are between the reflectors and the sources along these rays. We call this the daylight configuration.
3) The noise sources are spatially localized and the reflectors are between the sources and the sensors. We call this the backlight configuration, in analogy with photography.

We will show that imaging of reflectors can be done by migration of cross correlations. However, the migration imaging functional depends on the configuration of sources, sensors and reflectors. The stationary phase analysis in the next subsection makes clear which is the appropriate imaging functional in each configuration. This can also be done more informally using our understanding from Section 5 of how singular components appear in cross correlations. As noted in that section, the main contributions to the cross correlations $C^{(1)}(\tau, \mathbf{x}_1, \mathbf{x}_2)$ come from pairs of ray segments starting from a point in the noise source region and going through $\mathbf{x}_2$ and $\mathbf{x}_1$, respectively, with the same initial angle. When there is a reflector at $\mathbf{z}_\mathrm{r}$ then we must also consider rays that are reflected at $\mathbf{z}_\mathrm{r}$. Since the reflectors are assumed to be weak, the important pairs of ray segments are those with one direct ray and one

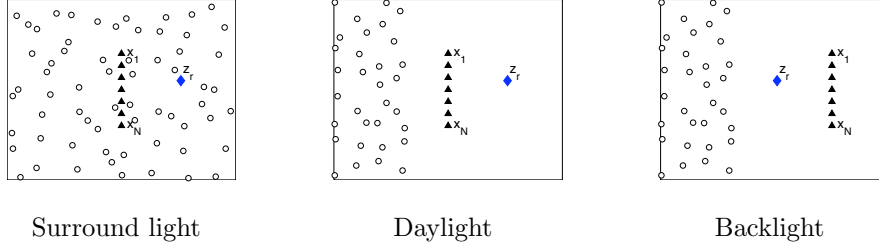Surround light   Daylight   Backlight

FIG. 6.1. *Left figure: The noise sources are distributed throughout the medium, which is the surround light imaging configuration. Middle figure: the sensors $(\mathbf{x}_j)_{j=1,\dots,N}$ are between the noise sources and the reflector $\mathbf{z}_r$, which is the daylight imaging configuration. Right figure: the reflector is between the noise sources and the sensors, which is the backlight imaging configuration.*
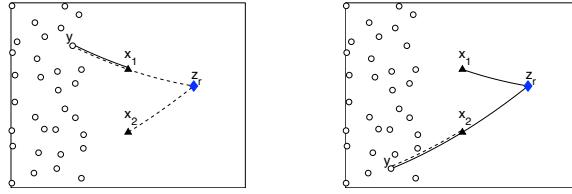

FIG. 6.2. *Pairs of ray segments that contribute to the singular component of the cross correlation of signals between $\mathbf{x}_1$ and $\mathbf{x}_2$ due to the reflector at $\mathbf{z}_r$, in a daylight configuration. The ray segments start from a point $\mathbf{y}$ in the noise source region with the same angle. One goes to $\mathbf{x}_1$ (solid) and the other one goes to $\mathbf{x}_2$ (dashed).*

broken ray going from the source region to $\mathbf{x}_1$ and $\mathbf{x}_2$, respectively. In the daylight configuration, the singular component of $C^{(1)}(\tau, \mathbf{x}_1, \mathbf{x}_2)$ due to the reflector comes from two pairs of ray segments, as shown in Figure 6.2. From this figure we see that the difference in travel times of the two ray segments is $\pm[\tau(\mathbf{x}_2, \mathbf{z}_r) + \tau(\mathbf{x}_1, \mathbf{z}_r)]$, with $+$ for the pair of ray segments in the left figure and $-$ for the pair of ray segments in the right figure. We show in Figure 6.3 two pairs of ray segments that contribute to the singular components of the cross correlation due to a reflector in the backlight configuration. From this figure we see that the differences in travel time of the two ray segments are $\tau(\mathbf{x}_2, \mathbf{z}_r) - \tau(\mathbf{x}_1, \mathbf{z}_r)$.

From these considerations we conclude that there is an important difference between daylight and backlight configurations. In daylight configurations the singular components of the cross correlations are concentrated at the total travel time $\tau(\mathbf{x}_2, \mathbf{z}_r) + \tau(\mathbf{x}_1, \mathbf{z}_r)$, while in backlight configurations they are concentrated at the difference travel time $\tau(\mathbf{x}_2, \mathbf{z}_r) - \tau(\mathbf{x}_1, \mathbf{z}_r)$. This determines the form of the migration imaging functional and its resolution.

6.2. Stationary phase analysis of the cross correlation with reflectors. We carry out the analysis when the background medium is smoothly varying and there is a point reflector at $\mathbf{z}_r$. Since we assume that the reflectors are weak, we use the Born approximation for the Green's function evaluated at high frequencies (see Appendix C):

$$\hat{G}\Big(\frac{\omega}{\varepsilon}, \mathbf{x}, \mathbf{y}\Big) = \hat{G}_0\Big(\frac{\omega}{\varepsilon}, \mathbf{x}, \mathbf{y}\Big) + \omega^2 \sigma_r \hat{G}_0\Big(\frac{\omega}{\varepsilon}, \mathbf{x}, \mathbf{z}_r\Big)\hat{G}_0\Big(\frac{\omega}{\varepsilon}, \mathbf{z}_r, \mathbf{y}\Big). \qquad (6.1)$$
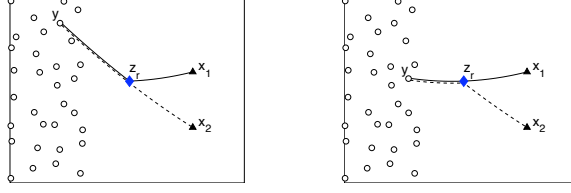
FIG. 6.3. *Same as in Figure 6.2 but in a backlight configuration.*

Here $\hat{G}_0$ is the Green's function (5.1) of the background medium, that is, in the absence of reflector, and $\sigma_{\rm r}$ is the reflectivity of the reflector.

PROPOSITION 6.1. *When there is a point reflector at $\mathbf{z}_{\rm r}$ with small reflectivity $\sigma_{\rm r}$ then the cross correlation $C^{(1)}(\tau, \mathbf{x}_1, \mathbf{x}_2)$ has two types of singular components, of order $O(1)$ and $O(\sigma_{\rm r})$ with respect to $\sigma_{\rm r}$, as described below.*

1) Terms of order $O(1)$:
If the ray going through $\mathbf{x}_1$ and $\mathbf{x}_2$ extends into the source region, that is, into the support of the function θ, then there are either one or two singular components at $\tau = \pm\tau(\mathbf{x}_1, \mathbf{x}_2)$.

2) Terms of order $O(\sigma_{\rm r})$:
If the ray going through $\mathbf{x}_1$ and $\mathbf{z}_{\rm r}$ extends into the source region and if $\mathbf{x}_1$ is between $\mathbf{z}_{\rm r}$ and the sources, then there is a singular component at $\tau = \tau(\mathbf{x}_1, \mathbf{z}_{\rm r}) + \tau(\mathbf{x}_2, \mathbf{z}_{\rm r})$.
If the ray going through $\mathbf{x}_1$ and $\mathbf{z}_{\rm r}$ extends into the source region and if $\mathbf{z}_{\rm r}$ is between $\mathbf{x}_1$ and the sources, then there is a singular component at $\tau = \tau(\mathbf{x}_2, \mathbf{z}_{\rm r}) - \tau(\mathbf{x}_1, \mathbf{z}_{\rm r})$.
If the ray going through $\mathbf{x}_2$ and $\mathbf{z}_{\rm r}$ extends into the source region and if $\mathbf{x}_2$ is between $\mathbf{z}_{\rm r}$ and the sources, then there is a singular component at $\tau = -\tau(\mathbf{x}_1, \mathbf{z}_{\rm r}) - \tau(\mathbf{x}_2, \mathbf{z}_{\rm r})$.
If the ray going through $\mathbf{x}_2$ and $\mathbf{z}_{\rm r}$ extends into the source region and if $\mathbf{z}_{\rm r}$ is between $\mathbf{x}_2$ and the sources, then there is a singular component at $\tau = \tau(\mathbf{x}_2, \mathbf{z}_{\rm r}) - \tau(\mathbf{x}_1, \mathbf{z}_{\rm r})$.

The non-singular components of order $O(1)$ of the cross correlation function $C^{(1)}(\tau, \mathbf{x}_1, \mathbf{x}_2)$ are supported in the interval $(-\tau(\mathbf{x}_1, \mathbf{x}_2), \tau(\mathbf{x}_1, \mathbf{x}_2))$ to leading order in ε.

The components of order $O(1)$ are the contributions of the direct waves that have not been scattered by the reflector at $\mathbf{z}_{\rm r}$. The components of order $O(\sigma_{\rm r})$ are the contributions of the waves that have been scattered by the reflector at $\mathbf{z}_{\rm r}$. In particular, in a daylight imaging configuration, there are singular components of order $O(\sigma_{\rm r})$ at $\tau = \pm(\tau(\mathbf{x}_1, \mathbf{z}_{\rm r}) + \tau(\mathbf{x}_2, \mathbf{z}_{\rm r}))$. In a backlight imaging configuration, there are a singular component of order $O(\sigma_{\rm r})$ at $\tau = \tau(\mathbf{x}_2, \mathbf{z}_{\rm r}) - \tau(\mathbf{x}_1, \mathbf{z}_{\rm r})$.

Proof. Using (6.1) and the WKB approximation, the Green's function has the form

$$\hat{G}\Big(\frac{\omega}{\varepsilon}, \mathbf{x}_1, \mathbf{x}_2\Big) \sim a(\mathbf{x}_1, \mathbf{x}_2)e^{i\frac{\omega}{\varepsilon}\tau(\mathbf{x}_1, \mathbf{x}_2)} + \omega^2 a_{\rm r}(\mathbf{x}_1, \mathbf{x}_2)e^{i\frac{\omega}{\varepsilon}\tau_{\rm r}(\mathbf{x}_1, \mathbf{x}_2)}. \qquad (6.2)$$

Here $\tau_{\rm r}(\mathbf{x}_1, \mathbf{x}_2)$ is the travel time from $\mathbf{x}_1$ to $\mathbf{x}_2$ with a reflection at $\mathbf{z}_{\rm r}$

$$\tau_{\rm r}(\mathbf{x}_1, \mathbf{x}_2) = \tau(\mathbf{x}_1, \mathbf{z}_{\rm r}) + \tau(\mathbf{z}_{\rm r}, \mathbf{x}_2),$$

and the corresponding amplitudes are $a(\mathbf{x}_1, \mathbf{x}_2)$ and $a_{\rm r}(\mathbf{x}_1, \mathbf{x}_2)$. The reflected amplitude a_r is much smaller than a since it is proportional to the reflectivity $\sigma_{\rm r}$ of the reflector at $\mathbf{z}_{\rm r}$.

Using (4.12) and the WKB approximation (6.2) of the Green's function we have, up to terms of order σ_{r},

$$C^{(1)}(\tau, \mathbf{x}_1, \mathbf{x}_2) \simeq C_{dd}^{(1)}(\tau, \mathbf{x}_1, \mathbf{x}_2) + C_{dr}^{(1)}(\tau, \mathbf{x}_1, \mathbf{x}_2) + C_{rd}^{(1)}(\tau, \mathbf{x}_1, \mathbf{x}_2),$$

with

$$C_{dd}^{(1)}(\tau, \mathbf{x}_1, \mathbf{x}_2) = \frac{1}{2\pi} \int d\mathbf{y}\theta(\mathbf{y}) \int d\omega \ \hat{F}(\omega) \overline{a}(\mathbf{x}_1, \mathbf{y}) a(\mathbf{x}_2, \mathbf{y}) e^{i\frac{\omega}{\varepsilon} \mathcal{T}_{dd}(\mathbf{y})},$$

$$C_{dr}^{(1)}(\tau, \mathbf{x}_1, \mathbf{x}_2) = \frac{1}{2\pi} \int d\mathbf{y}\theta(\mathbf{y}) \int d\omega \ \omega^2 \hat{F}(\omega) \overline{a}(\mathbf{x}_1, \mathbf{y}) a_{\mathrm{r}}(\mathbf{x}_2, \mathbf{y}) e^{i\frac{\omega}{\varepsilon} \mathcal{T}_{dr}(\mathbf{y})},$$

$$C_{rd}^{(1)}(\tau, \mathbf{x}_1, \mathbf{x}_2) = \frac{1}{2\pi} \int d\mathbf{y}\theta(\mathbf{y}) \int d\omega \ \omega^2 \hat{F}(\omega) \overline{a_{\mathrm{r}}}(\mathbf{x}_1, \mathbf{y}) a(\mathbf{x}_2, \mathbf{y}) e^{i\frac{\omega}{\varepsilon} \mathcal{T}_{rd}(\mathbf{y})}.$$

Here the subscript d denotes direct waves and r reflected waves. The rapid phases are given by

$$\omega\mathcal{T}_{dd}(\mathbf{y}) = \omega[\tau(\mathbf{y}, \mathbf{x}_2) - \tau(\mathbf{y}, \mathbf{x}_1) - \tau], \qquad\qquad (6.3)$$
$$\omega\mathcal{T}_{dr}(\mathbf{y}) = \omega[\tau(\mathbf{y}, \mathbf{x}_2) - \tau_{\mathrm{r}}(\mathbf{y}, \mathbf{x}_1) - \tau] = \omega[\tau(\mathbf{y}, \mathbf{x}_2) - \tau(\mathbf{y}, \mathbf{z}_{\mathrm{r}}) - \tau(\mathbf{z}_{\mathrm{r}}, \mathbf{x}_1) - \tau],$$
$$\omega\mathcal{T}_{rd}(\mathbf{y}) = \omega[\tau_{\mathrm{r}}(\mathbf{y}, \mathbf{x}_2) - \tau(\mathbf{y}, \mathbf{x}_1) - \tau] = \omega[\tau(\mathbf{y}, \mathbf{z}_{\mathrm{r}}) + \tau(\mathbf{z}_{\mathrm{r}}, \mathbf{x}_2) - \tau(\mathbf{y}, \mathbf{x}_1) - \tau].$$

The term $C_{dd}^{(1)}$ is of the same form as the function $C^{(1)}$ in the proof of Proposition 5.1. It has singular components only if $\mathbf{x}_1$, $\mathbf{x}_2$ and $\mathbf{y}$ are on the same ray. These singular components are supported on $\pm\tau(\mathbf{x}_1, \mathbf{x}_2)$ and they are of order $O(1)$.

The dominant contribution to the term $C_{dr}^{(1)}$ comes from the stationary points $(\omega, \mathbf{y})$ satisfying

$$\partial_\omega\left(\omega\mathcal{T}_{dr}(\mathbf{y})\right) = 0, \quad \nabla_{\mathbf{y}}\left(\omega\mathcal{T}_{dr}(\mathbf{y})\right) = \mathbf{0},$$

which gives the conditions

$$\tau(\mathbf{y}, \mathbf{x}_2) - \tau(\mathbf{y}, \mathbf{z}_{\mathrm{r}}) - \tau(\mathbf{z}_{\mathrm{r}}, \mathbf{x}_1) = \tau, \quad \nabla_{\mathbf{y}}\tau(\mathbf{y}, \mathbf{x}_2) = \nabla_{\mathbf{y}}\tau(\mathbf{y}, \mathbf{z}_{\mathrm{r}}).$$

By Lemma B.1 in the appendix, the second condition implies that $\mathbf{x}_2$ and $\mathbf{z}_{\mathrm{r}}$ are on the same side of a ray issuing from $\mathbf{y}$. If the points are aligned along the ray as $\mathbf{y} \to \mathbf{x}_2 \to \mathbf{z}_{\mathrm{r}}$, then the first condition is equivalent to $\tau = -\tau(\mathbf{z}_{\mathrm{r}}, \mathbf{x}_2) - \tau(\mathbf{z}_{\mathrm{r}}, \mathbf{x}_1)$. If the points are aligned along the ray as $\mathbf{y} \to \mathbf{z}_{\mathrm{r}} \to \mathbf{x}_2$, then the first condition is equivalent to $\tau = \tau(\mathbf{z}_{\mathrm{r}}, \mathbf{x}_2) - \tau(\mathbf{z}_{\mathrm{r}}, \mathbf{x}_1)$. The analysis of the term $C_{rd}^{(1)}$ goes along the same lines. The terms $C_{dr}^{(1)}$ and $C_{rd}^{(1)}$ are both of order $O(\sigma_{\mathrm{r}})$.

The last statement of the proposition concerns the support of the non-singular component of the cross correlation C_{dd}, which represents the contributions of the direct waves. Even without applying the stationary phase method, information about the support of C_{dd} can be obtained from the form (6.3) of $\mathcal{T}_{dd}(\mathbf{y})$ and the triangle inequality $|\tau(\mathbf{y}, \mathbf{x}_1) - \tau(\mathbf{y}, \mathbf{x}_2)| \leq \tau(\mathbf{x}_1, \mathbf{x}_2)$. Therefore, the support of C_{dd} as a function of τ is in the interval $(-\tau(\mathbf{x}_1, \mathbf{x}_2), \tau(\mathbf{x}_1, \mathbf{x}_2))$. $\qquad\square$

6.3. Migration imaging of cross correlations. In order to image the reflectors, we first assume that we know the medium, in the sense that the travel times between the sensors and points in the region around the reflectors to be imaged are known. If in particular the medium is homogeneous then $\tau(\mathbf{x}, \mathbf{y}) = |\mathbf{x} - \mathbf{y}|/c_0$.

The primary data for imaging is the set $\{C(\tau, \mathbf{x}_j, \mathbf{x}_l)\}$, $j, l = 1, \ldots, N$, of cross correlation of signals recorded at the sensors located at $\mathbf{x}_j$, $j = 1, \ldots, N$. Even when the signal to noise ratio (SNR) at the sensors is large, this primary data set cannot be used directly for imaging because peaks in the cross correlations due to the reflectors are very weak compared both to the peaks of the direct waves and to the non-singular components due to the directional energy flux. It is therefore necessary to process the cross correlations before migration imaging.

There are two ways to process the primary cross correlations:
1) If data sets $\{C\}$ and $\{C_0\}$ with and without the reflectors, respectively, are available then we can compute the *differential* cross correlations $\{C - C_0\}$ at the sensors and migrate them. This takes out noise source and sensor location effects regardless of the type of illumination.
2) If only the data set $\{C\}$ with the reflectors is available then we can mask the part of the cross correlations in the interval between travel times among the sensors. This includes elimination of the main peaks at the travel times between sensors. We refer to the resulting masked cross correlations as *coda* cross correlations, $\{C_{\mathrm{coda}}\}$.

The form of the migration imaging functional for both differential and coda cross correlations depends in an essential way on the type of illumination as explained in the next subsection.

6.4. Migration imaging with daylight illumination. We consider first migration of differential cross correlations in a daylight illumination configuration. The Kirchhoff migration (KM) imaging functional at a search point $\mathbf{z}^S$ is the daylight imaging functional

$$\mathcal{I}^{\mathrm{D}}(\mathbf{z}^S) = \sum_{j,l=1}^{N} \left[C^{\mathrm{sym}} - C_0^{\mathrm{sym}} \right] \left(\tau(\mathbf{z}^S, \mathbf{x}_l) + \tau(\mathbf{z}^S, \mathbf{x}_j), \mathbf{x}_j, \mathbf{x}_l \right), \qquad (6.4)$$

where we have defined $C^{\mathrm{sym}}(\tau, \mathbf{x}_j, \mathbf{x}_l) = [C(\tau, \mathbf{x}_j, \mathbf{x}_l) + C(-\tau, \mathbf{x}_j, \mathbf{x}_l)]\mathbf{1}_{(0,\infty)}(\tau)$, and similarly for $C_0^{\mathrm{sym}}(\tau, \mathbf{x}_j, \mathbf{x}_l)$. This functional uses the positive and negative parts of the cross correlations, which correspond to the causal and anti-causal Green's functions, and back-propagates them. It is a consequence of the stationary phase analysis of Proposition 6.1 that the argument of the imaging functional should be chosen at the sum of the travel times $\tau(\mathbf{z}^S, \mathbf{x}_l) + \tau(\mathbf{z}^S, \mathbf{x}_j)$. Indeed it is shown there that $C - C_0$ has singular components at $\pm[\tau(\mathbf{z}_{\mathrm{r}}, \mathbf{x}_l) + \tau(\mathbf{z}_{\mathrm{r}}, \mathbf{x}_j)]$.

Migration imaging of coda cross correlations with daylight illumination is entirely analogous. The daylight imaging functional at a search point $\mathbf{z}^S$ is

$$\mathcal{I}^{\mathrm{D}}(\mathbf{z}^S) = \sum_{j,l=1}^{N} C_{\mathrm{coda}}^{\mathrm{sym}} \left(\tau(\mathbf{z}^S, \mathbf{x}_j) + \tau(\mathbf{z}^S, \mathbf{x}_l), \mathbf{x}_j, \mathbf{x}_l \right), \qquad (6.5)$$

where now $C_{\mathrm{coda}}^{\mathrm{sym}}(\tau, \mathbf{x}_j, \mathbf{x}_l) = [C(\tau, \mathbf{x}_j, \mathbf{x}_l) + C(-\tau, \mathbf{x}_j, \mathbf{x}_l)]\mathbf{1}_{(\tau(\mathbf{x}_j, \mathbf{x}_l), \infty)}(\tau)$. By removing the central part of the cross correlation function, we remove the singular and non-singular contributions of the direct waves that are large and essentially concentrated in the interval $(-\tau(\mathbf{x}_j, \mathbf{x}_l), \tau(\mathbf{x}_j, \mathbf{x}_l))$, as shown in Proposition 6.1. However, we do not remove the interesting singular component at (plus or minus) the sum of travel times $\tau(\mathbf{z}_{\mathrm{r}}, \mathbf{x}_l) + \tau(\mathbf{z}_{\mathrm{r}}, \mathbf{x}_j)$ due to the waves that have been scattered by the reflector, because the triangle inequality ensures that $\tau(\mathbf{z}_{\mathrm{r}}, \mathbf{x}_l) + \tau(\mathbf{z}_{\mathrm{r}}, \mathbf{x}_j) > \tau(\mathbf{x}_j, \mathbf{x}_l)$ (except in the very unlikely case when $\mathbf{z}_r$ is along the segment between $\mathbf{x}_j$ and $\mathbf{x}_l$). Therefore by removing this central part, the imaging functional has essentially the same behavior

as the one using differential cross correlations. In practice, the coda truncation should be done with a small margin beyond the travel time $\tau(\mathbf{x}_j, \mathbf{x}_l)$, roughly equal to a few times the background speed times the decoherence time.

The daylight imaging functional (6.4) (or (6.5)) has the same form as the KM imaging functional that is used when the reflectors are illuminated by active sensors at $(\mathbf{x}_j)_{j=1,\ldots,N}$ and the data is the response matrix $P(t, \mathbf{x}_l, \mathbf{x}_j)$. The sensor at $\mathbf{x}_j$ emits an impulse with a specified bandwidth, the sensor at $\mathbf{x}_l$ records the signal $P(t, \mathbf{x}_l, \mathbf{x}_j)$, and the KM migration functional is

$$\mathcal{I}^{\mathrm{KM}}(\mathbf{z}^S) = \sum_{j,l=1}^{N} P\big(\tau(\mathbf{z}^S, \mathbf{x}_j) + \tau(\mathbf{z}^S, \mathbf{x}_l), \mathbf{x}_j, \mathbf{x}_l\big). \tag{6.6}$$

It is remarkable that daylight migration imaging with passive sensor cross correlations is essentially equivalent to migration imaging with active sensors.

A resolution analysis of migration imaging with active sensor arrays has been carried out in detail [6, 7]. It applies directly to migration imaging with cross correlations as introduced here. We see that the cross range resolution for a linear sensor array with aperture a is given by $\lambda a/L$. Here L is the distance between the sensor array and the reflectors and λ is the central wavelength. The range resolution is proportional to the background velocity times the inverse of the bandwidth.

In Figure 6.4 we show the results of numerical simulations for a sparse array of 5 sensors and with one reflector. There are 200 point noise sources distributed over the domain $[-50, 50] \times [0, 15]$. The power spectral density of the noise sources is a Gaussian $\exp(-\omega^2/2)$. The speed and the bandwidth are normalized to one so that the range resolution is also normalized to one. The image window is 40×40 range resolutions. It is clear that passive imaging with coda cross correlations gives very good results.

6.5. Migration imaging with backlight illumination. We consider first migration imaging with backlight illumination when we have differential cross correlation sensor data $\{C - C_0\}$. The backlight imaging functional at a search point $\mathbf{z}^S$ is

$$\mathcal{I}^{\mathrm{B}}(\mathbf{z}^S) = \sum_{j,l=1}^{N} \big[C - C_0\big]\big(\tau(\mathbf{z}^S, \mathbf{x}_l) - \tau(\mathbf{z}^S, \mathbf{x}_j), \mathbf{x}_j, \mathbf{x}_l\big). \tag{6.7}$$

The signs of the travel times in the argument of the imaging functional are determined by Proposition 6.1. It is shown there that the singular component of $(C - C_0)(\tau, \mathbf{x}_j, \mathbf{x}_l)$ due the waves that have been reflected by the reflector is at $\tau = \tau(\mathbf{z}_{\mathrm{r}}, \mathbf{x}_l) - \tau(\mathbf{z}_{\mathrm{r}}, \mathbf{x}_j)$.

We note that (6.7) in the Fourier domain has the form

$$\mathcal{I}^{\mathrm{B}}(\mathbf{z}^S) = \frac{1}{2\pi} \int d\omega \sum_{j,l=1}^{N} e^{-i\omega[\tau(\mathbf{z}^S, \mathbf{x}_l) - \tau(\mathbf{z}^S, \mathbf{x}_j)]} \big[\hat{C} - \hat{C}_0\big](\omega, \mathbf{x}_j, \mathbf{x}_l),$$

which is the same as the incoherent interferometric imaging functional that is used when $\mathbf{z}_{\mathrm{r}}$ is a source emitting an impulse that is recorded by passive sensors at $(\mathbf{x}_j)_{j=1,\ldots,N}$ and the data is the vector $P(t, \mathbf{x}_j)$. The incoherent interferometric func-
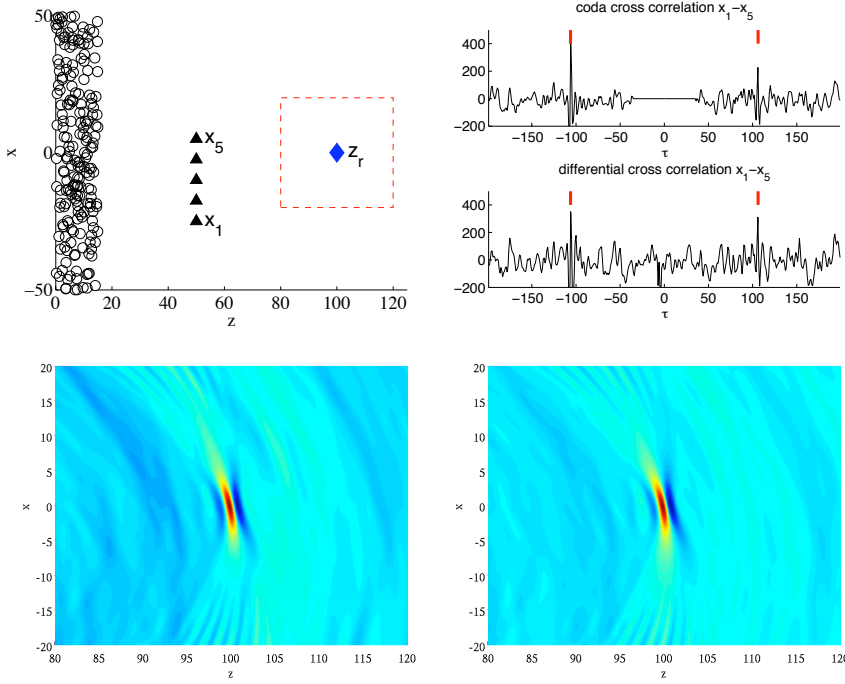
Fig. 6.4. *Numerical simulations for daylight migration imaging with an array of five passive sensors (triangles on the top left figure). The reflector to be imaged (diamond) is located at ($x_r = 0, z_r = 100$) and is illuminated by noise sources (circles). The coda correlation and the differential correlation of the signals recorded by the two sensors at the ends of the array are shown at the top right figure. The migration imaging functional (6.4) using differential cross correlations is shown at the bottom left figure. Migration imaging with coda cross correlations (6.5) is shown at the bottom right figure. Here the image window in which $\mathbf{z}^S$ varies is 40×40 range resolution units around the reflector.*

tional (IINT) has the form

$$\mathcal{I}^{\text{IINT}}(\mathbf{z}^S) = \frac{1}{2\pi} \int d\omega \Big| \sum_{l=1}^{N} e^{-i\omega\tau(\mathbf{z}^S, \mathbf{x}_l)} \hat{P}(\omega, \mathbf{x}_l) \Big|^2$$

$$= \frac{1}{2\pi} \int d\omega \sum_{j,l=1}^{N} e^{-i\omega[\tau(\mathbf{z}^S, \mathbf{x}_l) - \tau(\mathbf{z}^S, \mathbf{x}_j)]} \hat{P}(\omega, \mathbf{x}_l)\overline{\hat{P}(\omega, \mathbf{x}_j)}$$

and is identical to a matched field imaging functional. A resolution analysis of it has already been carried out [7] and can be directly used here. We see that backlight cross correlation imaging with passive sensor arrays does not provide any range resolution, as in incoherent interferometric imaging. When the sensors are distributed or when the array is large then range resolution can be obtained by geometric triangulation.

Let us consider backlight imaging when we only have data in the presence of reflectors. The main contribution of the reflector in the cross correlation $C(\tau, \mathbf{x}_j, \mathbf{x}_l)$ is at $\tau = \tau(\mathbf{z}_r, \mathbf{x}_l) - \tau(\mathbf{z}_r, \mathbf{x}_j)$. It is buried in the interval $(-\tau(\mathbf{x}_j, \mathbf{x}_l), \tau(\mathbf{x}_j, \mathbf{x}_l))$ that contains the contributions of the direct waves from the noise sources. This is because of the triangular inequality $|\tau(\mathbf{z}_r, \mathbf{x}_l) - \tau(\mathbf{z}_r, \mathbf{x}_j)| \leq \tau(\mathbf{x}_j, \mathbf{x}_l)$. Therefore it is impossible to use masking so as to amplify the effect of the reflectors. The only thing that can
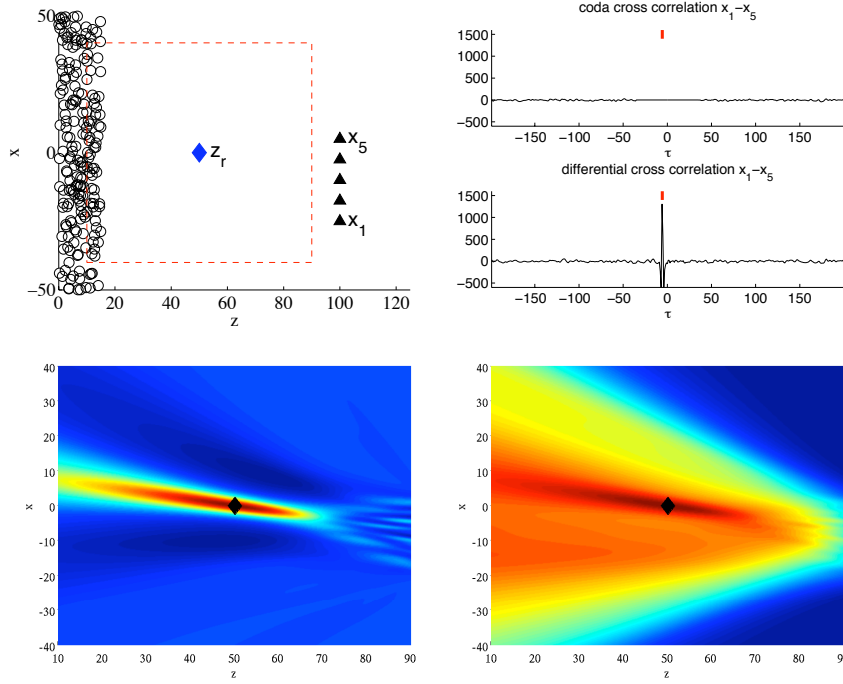
FIG. 6.5. *Numerical simulations for backlight migration imaging with an array of five passive sensors (triangles on the top left figure). The reflector to be imaged (diamond) is located at $(x_r = 0, z_r = 50)$ and is illuminated by noise sources (circles). The coda correlation and the differential correlation of the signals recorded by the two sensors at the ends of the array are shown at the top right figure. The migration imaging functional (6.7) using differential cross correlations is shown at the bottom left figure. It is not possible to use the coda cross correlation here as was done with daylight imaging in Figure 6.4. Now we back propagate the full cross correlation function with formula (6.8) and we get the bottom right figure. The search window is 80×80 range resolution units around the reflector.*

be done is to back propagate the full cross correlations. The KM imaging functional at a search point $\mathbf{z}^S$ has the form

$$\mathcal{I}^{\mathrm{B}}(\mathbf{z}^S) = \sum_{j,l=1}^{N} C\big(\tau(\mathbf{z}^S, \mathbf{x}_l) - \tau(\mathbf{z}^S, \mathbf{x}_j), \mathbf{x}_j, \mathbf{x}_l\big).$$

We see in Figure 6.5 that the quality of this image is inferior to the one obtained with the functional (6.7) using differential cross correlations, even though the scattering coefficient has been increased in this case compared to the previous ones.

6.6. Migration imaging with surround light illumination. With surround light illumination the noise sources are distributed everywhere around the passive sensors and the reflectors. The imaging functional (6.4) with differential cross correlations has the same properties as in the one with daylight illumination. Similarly, the imaging functional (6.7) has the same properties as the one with backlight illumination. Therefore both imaging functionals can be used so as to possibly enhance the signal to noise ratio. However the daylight imaging functional (6.4) has a much better range resolution than (6.7) and so it should be used exclusively if possible. In migration

imaging with coda cross correlations it is clearly preferable to use the daylight imaging functional (6.5).

We note that when imaging with cross correlations it may also be possible to estimate the propagation speed of the background medium when it is not known but is smoothly varying. The sensor array must in such cases be distributed in a suitable way in the region of interest. We must first use the cross correlations to estimate travel times between sensors. Then we can estimate the background velocity with a least squares tomographic method [3]. Migration imaging can now be done with travel times based on the estimated background velocity.

7. Passive sensor imaging with cross correlations in a scattering medium. In this section we consider imaging by cross correlations, as in the previous section, but in addition to the smoothly varying background speed there are random inhomogeneities that cause multiple scattering. There are both advantages and disadvantages when imaging reflectors in such an environment. One important advantage is that even localized noise sources can appear to have considerably enhanced directional diversity because of the scattering medium. An inevitable disadvantage is loss of resolution and blurring because of the environmental inhomogeneities.

A qualitative way to assess this trade-off is by using the transport mean free path as a measure of distances over which coherent wave propagation transforms into incoherent wave energy transport. Coherent sensor imaging as introduced in the previous section cannot be expected to work unless distances between sensors and reflectors are of the order of the transport mean free path or shorter. It is also expected that the directional diversity of the noise sources will be enhanced if the distances between sensors and reflectors to noise sources are large compared to the transport mean free path. Under these circumstances, coherent sensor imaging will benefit from enhanced directional diversity of the noise sources without too much loss of resolution and blurring.

7.1. Structure of the cross correlation in a scattering medium. There are two different contributions in the empirical cross correlations $C_T(\tau, \mathbf{x}_1, \mathbf{x}_2)$, in addition to the singular component at $\tau = \pm\tau(\mathbf{x}_1, \mathbf{x}_2)$ corresponding to the direct waves from the noise sources.

One contribution comes from the residual fluctuations of the noise sources, which emit stationary random signals. The empirical correlations C_T are random functions with standard deviation of order $T^{-1/2}$, as described in Appendix A. These fluctuations decay as the integration time T becomes larger. The other contribution comes from the multiple scattering of waves by the inhomogeneities in the environment. These contributions are there because even though the identity (2.2) may not hold exactly when there is not enough directional diversity, the cross correlations contain information beyond an estimate of the travel time between the sensors. We expect that for T large, the tails of C_T capture approximately the tails of the Green's function that are generated by the scattered waves. The tails of C_T contain information about both coherent waves, due the reflectors that we want to image, as well as incoherent superpositions of waves multiply scattered by the random inhomogeneities.

In the remainder of this section we assume that the integration time T is large enough so that the residual fluctuations from the noise sources are negligible compared to those from multiple scattering.

7.2. Iterated cross correlations and coherent interferometry. As in the case of imaging in a smoothly varying medium discussed in Section 6, the sensor cross
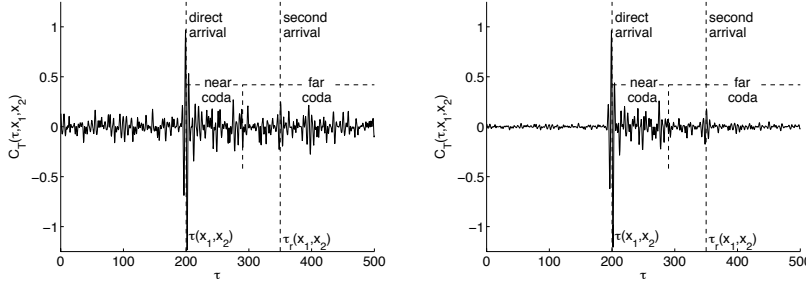
FIG. 7.1. *Schematic of typical forms of the empirical cross correlation $C_T(\tau, \mathbf{x}_1, \mathbf{x}_2)$ in a scattering medium, with a reflector embedded in it at $\mathbf{z}_r$. We see clearly the singular component at lag time $\tau = \tau(\mathbf{x}_1, \mathbf{x}_2)$, corresponding to the direct waves from the noise sources. We also see a smaller singular component at lag time $\tau = \tau_r(\mathbf{x}_1, \mathbf{x}_2) = \tau(\mathbf{z}_r, \mathbf{x}_1) + \tau(\mathbf{z}_r, \mathbf{x}_2)$, corresponding to the waves reflected at $\mathbf{z}_r$. The coda beyond $\tau = \tau(\mathbf{x}_1, \mathbf{x}_2)$ comes from waves scattered by the random inhomogeneities of the medium. The near coda is dominated by single-scattered waves while the far coda is due to multiply-scattered waves. These components can be identified if the integration time T is long enough so that the residual fluctuations from the noise sources are small. This is the case on the right figure but not on the left one.*

correlations $\{C(\tau, \mathbf{x}_j, \mathbf{x}_l), \, j, l = 1, \ldots, N\}$ need to be processed in order to amplify the contribution of the reflectors. We assume here that we have sensor data in the same environment in the absence of the reflectors, and for simplicity we let C stand for differential cross correlations. It is unlikely that imaging in a scattering environment can be done without having differential cross correlations. We need to take out the effects of the environment as much as possible if migration in a fictitious, smoothly varying background is to be at all successful.

We noted in Subsection 6.4, below equation (6.6), that with favorable illumination the passive sensor cross correlations, or differential cross correlations, provide an estimate for the bandlimited impulse response, or differential impulse response, of an equivalent active sensor network. This is true in a smoothly varying background and in the presence of weak scatterers when the single scattering approximation can be used, as we show in a similar context in Section 8. It is expected to be true even with strong multiple scattering but coherent sensor imaging in such an environment is unlikely to be successful.

Assuming that the passive sensor differential cross correlations provide a good estimate of the equivalent active sensor differential impulse response, we can implement the coherent interferometric imaging techniques (CINT) developed for active sensors [8]. The key idea in CINT is to migrate cross correlations of the impulse response, rather than the impulse response itself. In the present context this translates into migrating cross correlations of the differential cross correlations $C(\tau, \mathbf{x}_j, \mathbf{x}_l)$, which means that we use fourth-order cross correlations. It is important, however, to compute these fourth order cross correlations *locally* in time and space, and not over the whole time interval and the whole set of pairs of sensors, as we now explain.

In the time domain, the components of the cross correlations $C(\tau, \mathbf{x}_j, \mathbf{x}_l)$ associated with the reflectors do not appear as clean peaks at travel times corresponding to those between sensors and reflectors. They have, in addition, codas generated by the inhomogeneities of the scattering medium. The typical duration of such a coda is called delay spread. We segment the cross correlations $C(\tau, \mathbf{x}_j, \mathbf{x}_l)$ into time intervals and compute their cross correlations locally in each interval. The width T_d of the

time intervals should be chosen to be comparable to the delay spread. If T_d is small compared to the delay spread, then the fourth order local cross correlations cannot compress the coda and the images have speckles. If T_d is large compared to the delay spread, then the images are smooth but there is too much loss of resolution and blurring. However, the delay spread is usually not known since it depends on the random medium. It is shown in [7] that the reciprocal of the delay spread is proportional to the decoherence frequency of the Fourier transform of $C(\tau, \mathbf{x}_j, \mathbf{x}_l)$. Therefore, the delay spread could be estimated by exploiting this remark, and then used to determine the time windows over which local fourth order cross correlations are computed. It is more efficient, and the images have better resolution, if we choose the width T_d of the time intervals adaptively, as we discuss at the end of this subsection. Given T_d, the CINT daylight imaging functional has the form

$$\mathcal{I}^{\mathrm{CINT}}(\mathbf{z}^S) = \sum_{j,j',l,l'=1}^{N} \iint_{|\omega-\omega'|\leq T_d^{-1}} \hat{C}(\omega,\mathbf{x}_j,\mathbf{x}_l)\overline{\hat{C}}(\omega',\mathbf{x}_{j'},\mathbf{x}_{l'})$$
$$\times e^{-i\omega[\tau(\mathbf{x}_j,\mathbf{z}^S)+\tau(\mathbf{x}_l,\mathbf{z}^S)]}e^{i\omega'[\tau(\mathbf{x}_{j'},\mathbf{z}^S)+\tau(\mathbf{x}_{l'},\mathbf{z}^S)]}d\omega d\omega'. \quad (7.1)$$

We can compare this expression to the square of the daylight imaging functional (6.4), which has the form

$$\left|\mathcal{I}^{\mathrm{D}}(\mathbf{z}^S)\right|^2 = \sum_{j,j',l,l'=1}^{N} \iint \hat{C}(\omega,\mathbf{x}_j,\mathbf{x}_l)\overline{\hat{C}}(\omega',\mathbf{x}_{j'},\mathbf{x}_{l'})$$
$$\times e^{-i\omega[\tau(\mathbf{x}_j,\mathbf{z}^S)+\tau(\mathbf{x}_l,\mathbf{z}^S)]}e^{i\omega'[\tau(\mathbf{x}_{j'},\mathbf{z}^S)+\tau(\mathbf{x}_{l'},\mathbf{z}^S)]}d\omega d\omega', \quad (7.2)$$

where we recall that here C stands for differential cross correlation. We see that the CINT imaging functional (7.1) and the square of the KM functional (7.2) differ only in that the frequencies $|\omega - \omega'| > T_d^{-1}$, where fourth order correlations are weak, are eliminated in CINT.

It is often possible to go one step further in specializing the CINT imaging functional in the case of passive sensor arrays. There is a characteristic decoherence length in the spatial domain, which is similar to the decoherence frequency. This decoherence length X_d is the distance between sensors beyond which the coda that can be recorded at them are not correlated. The cross correlations of such coda tend to increase the fluctuations of the imaging functional. We therefore remove them. The resulting CINT imaging functional at a search point $\mathbf{z}^S$ has the form

$$\mathcal{I}^{\mathrm{CINT}}(\mathbf{z}^S) = \sum_{\substack{l,j,l',j'=1 \\ |\mathbf{x}_j-\mathbf{x}_{j'}|\leq X_d, |\mathbf{x}_l-\mathbf{x}_{l'}|\leq X_d}}^{N} \iint_{|\omega-\omega'|\leq T_d^{-1}} d\omega d\omega' \hat{C}(\omega,\mathbf{x}_j,\mathbf{x}_l)\overline{\hat{C}}(\omega',\mathbf{x}_{j'},\mathbf{x}_{l'})$$
$$\times e^{-i\omega[\tau(\mathbf{x}_j,\mathbf{z}^S)+\tau(\mathbf{x}_l,\mathbf{z}^S)]}e^{i\omega'[\tau(\mathbf{x}_{j'},\mathbf{z}^S)+\tau(\mathbf{x}_{l'},\mathbf{z}^S)]}.$$

Note that the decoherence length can be very small (of the order of the wavelength) when random scattering is very strong [8], and this means that only diagonal terms $j = j'$ and $l = l'$ should be kept in this case. After a change of variables it can be seen more clearly that the fourth order cross correlations are computed only over nearby

frequencies and sensors:

$$\mathcal{I}^{\mathrm{CINT}}(\mathbf{z}^S) = \sum_{\substack{j,j'=1\\|\mathbf{x}_j-\mathbf{x}_{j'}|\leq X_d}}^{N} \sum_{\substack{l,l'=1\\|\mathbf{x}_l-\mathbf{x}_{l'}|\leq X_d}}^{N} \iint_{|\Omega|\leq T_d^{-1}} d\Omega d\omega$$

$$\times \hat{C}\big(\omega + \frac{\Omega}{2},\mathbf{x}_j,\mathbf{x}_l\big)\overline{\hat{C}}\big(\omega - \frac{\Omega}{2},\mathbf{x}_{j'},\mathbf{x}_{l'}\big) e^{-i\frac{\omega}{2}[\tau(\mathbf{x}_j,\mathbf{z}^S)-\tau(\mathbf{x}_{j'},\mathbf{z}^S)]}$$

$$\times e^{-i\frac{\omega}{2}[\tau(\mathbf{x}_l,\mathbf{z}^S)-\tau(\mathbf{x}_{l'},\mathbf{z}^S)]-i\frac{\Omega}{2}[\tau(\mathbf{x}_j,\mathbf{z}^S)+\tau(\mathbf{x}_{j'},\mathbf{z}^S)]-i\frac{\Omega}{2}[\tau(\mathbf{x}_l,\mathbf{z}^S)+\tau(\mathbf{x}_{l'},\mathbf{z}^S)]}\,.$$

It is shown in [8] that the range resolution of CINT is of the order of T_d times the background speed and the cross range resolution of the order of $\lambda L/X_d$.

An adaptive procedure for estimating optimally the unknown parameters T_d and X_d is based on minimizing a suitable norm of the image to improve its quality, both in terms of resolution and signal-to-noise ratio. This norm should penalize speckle fluctuations and also should minimize blurring. A possible choice [8] is a sum of the L^1 norm of the functional and of the L^1 norm of the gradient of the normalized functional $\sqrt{|\mathcal{I}^{\mathrm{CINT}}(\mathbf{z}^S)|}/\sup_{\mathbf{z}} \sqrt{|\mathcal{I}^{\mathrm{CINT}}(\mathbf{z})|}$. This normalization is chosen so that when there is no smoothing, $X_d \to \infty$ and $T_d^{-1} \to \infty$, then we recover the KM functional.

8. Iterated cross correlations for travel time estimation in a weakly scattering medium. For travel time tomography to be successful it is necessary to have good estimates of the travel times between pairs of sensors that cover well the region of interest. When the noise sources are spatially localized and there is a strong directional energy flux at the sensors, then travel time estimates will be poor for sensor pairs in directions perpendicular to this flux. In this section we show that it is possible to exploit scattering from random inhomogeneities so as to enhance travel time estimation.

8.1. The use of auxiliary sensors. We consider distributions of noise sources that are spatially localized and media with scattering that is not strong enough for equipartition of the fields at the sensors [34]. Therefore, even with scattering, the signals depend strongly on the spatial localization of the noise sources, which affects the quality of travel time estimation. However, the coda of the cross correlations are generated by scattered waves, which have more directional diversity than the direct waves from the noise sources. By cross correlating the coda of the cross correlations, which produces fourth order cross correlations, it is possible to exploit scattered waves and their enhanced directional diversity. Campillo and Stehly [13] suggest a way to estimate the Green's function between $\mathbf{x}_1$ and $\mathbf{x}_2$ as follows.

1) Calculate the cross correlations between $\mathbf{x}_1$ and $\mathbf{x}_{\mathrm{a},j}$ and between $\mathbf{x}_2$ and $\mathbf{x}_{\mathrm{a},j}$ for a large number N of auxiliary sensors $(\mathbf{x}_{\mathrm{a},j})_{j=1,\dots,N}$ that are distributed over the medium

$$C_T(\tau,\mathbf{x}_{\mathrm{a},j},\mathbf{x}_l) = \frac{1}{T}\int_0^T u(t,\mathbf{x}_{\mathrm{a},j})u(t+\tau,\mathbf{x}_l)dt\,, \quad l=1,2\,.$$

2) Cross correlate the coda (i.e. the tails) of these cross correlations and sum them over all auxiliary sensors to form the coda cross correlation between $\mathbf{x}_1$ and $\mathbf{x}_2$:

$$C_{T',T}(\tau,\mathbf{x}_1,\mathbf{x}_2) = \sum_{j=1}^{N} \int_{[-T',-T_{\mathrm{coda}}]\cup[T_{\mathrm{coda}},T']} C_T(\tau',\mathbf{x}_{\mathrm{a},j},\mathbf{x}_1)C_T(\tau'+\tau,\mathbf{x}_{\mathrm{a},j},\mathbf{x}_2)d\tau'\,.$$
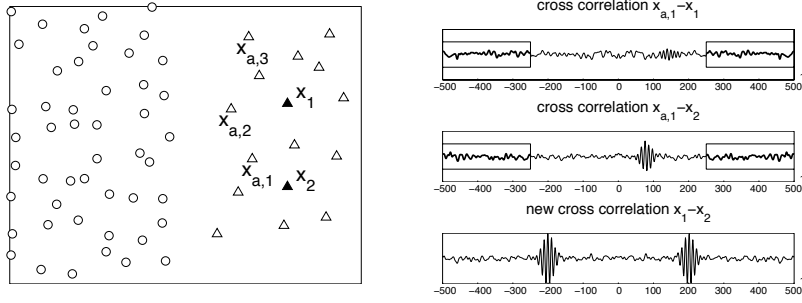
$$(8.1)$$

FIG. 8.1. *When noise sources (circles in the left figure) are spatially localized, we form cross correlations between the recorded signals at $\mathbf{x}_1$ and $\mathbf{x}_2$ (solid triangles) and those at auxiliary sensors at $\mathbf{x}_{a,j}$ (empty triangles). We then compute cross correlations of the tails of these correlations (here, $T_{\mathrm{coda}} = 250$) and sum over the auxiliary sensors. This gives the coda cross correlation (8.1) from which the travel time between $\mathbf{x}_1$ and $\mathbf{x}_2$ can be better estimated, as indicated in the schematic figure on the right.*

Here the time T_{coda} is chosen so as to eliminate the coherent part of C_T. In general, T_{coda} should be larger than $\max(\tau(\mathbf{x}_{a,j}, \mathbf{x}_1), \tau(\mathbf{x}_{a,j}, \mathbf{x}_2))$.

Using the stationary phase method we show in the next subsections that the algorithm proposed by Campillo and Stehly can exploit the enhanced directivity of scattered waves. We show in particular that the coda cross correlation $C_{T',T}$, defined by (8.1), has singular components at the travel time between the sensors even in the unfavorable case in which the ray joining $\mathbf{x}_1$ and $\mathbf{x}_2$ does not reach into the source region, as discussed in Section 5.

8.2. A model for the scattering medium and the auxiliary sensors. In order to analyze the coda (fourth-order) cross correlation (8.1) we first introduce a model for the inhomogeneous medium. A simple single-scattering model is sufficient for this purpose. We assume that the medium has of a smoothly varying background speed $c_0(\mathbf{x})$, which we want to image, and a large collection of point scatterers at $(\mathbf{z}_{s,j})_{j \geq 1}$. Their reflectivities σ_j are assumed to be zero-mean independent random variables with small variance σ^2. In the Born (single-scattering) approximation (see Appendix C) the full Green's function at scaled high frequencies is given by

$$\hat{G}\left(\frac{\omega}{\varepsilon}, \mathbf{x}, \mathbf{y}\right) = \hat{G}_0\left(\frac{\omega}{\varepsilon}, \mathbf{x}, \mathbf{y}\right) + \hat{G}_1\left(\frac{\omega}{\varepsilon}, \mathbf{x}, \mathbf{y}\right), \tag{8.2}$$

where $\hat{G}_0$ is the Green's function (5.1) of the background medium and $\hat{G}_1$ is given by

$$\hat{G}_1\left(\frac{\omega}{\varepsilon}, \mathbf{x}, \mathbf{y}\right) = \omega^2 \sum_j \sigma_j \hat{G}_0\left(\frac{\omega}{\varepsilon}, \mathbf{x}, \mathbf{z}_{s,j}\right) \hat{G}_0\left(\frac{\omega}{\varepsilon}, \mathbf{z}_{s,j}, \mathbf{y}\right). \tag{8.3}$$

We also assume that:
1) The auxiliary sensors at $(\mathbf{x}_{a,j})_{j=1,\dots,N}$ are distributed with a continuum density $\chi(\mathbf{x}_a)$. This means that we can approximate sums over the auxiliary sensors by integrals with density χ:

$$\sum_j \psi(\mathbf{x}_{a,j}) \simeq \int d\mathbf{x}_a \chi(\mathbf{x}_a) \psi(\mathbf{x}_a), \tag{8.4}$$

for any real-valued test function ψ.

2) The scatterers at $(\mathbf{z}_{s,j})_{j\geq 1}$ are distributed with a continuum density $\rho(\mathbf{z}_s)$. Since the reflectivities σ_j are zero-mean independent random variables with variance σ^2, by the central limit theorem we can approximate the distribution of vectors by a Gaussian

$$\left(\sum_j \sigma_j \psi_1(\mathbf{z}_{s,j}), \ldots, \sum_j \sigma_j \psi_n(\mathbf{z}_{s,j}) \right) \simeq \mathcal{N}\left(0, Q\right), \tag{8.5}$$

for any real-valued test functions $\psi_1, \ldots, \psi_n$. Here $\mathcal{N}(0, Q)$ stands for the multivariate normal distribution with zero-mean and covariance matrix Q given by

$$Q_{jl} = \sigma^2 \int d\mathbf{z}_s \rho(\mathbf{z}_s) \psi_j(\mathbf{z}_s) \psi_l(\mathbf{z}_s).$$

8.3. Stationary phase analysis for fourth-order cross correlations. We distinguish two components in the cross correlation function $C^{(1)}$ defined by (4.10):

1) The coherent component $C^{(1)}_{\mathrm{coh}}$ is associated with the direct waves that have not been scattered. From the representation (8.2) of the Green's function, the coherent component $C^{(1)}_{\mathrm{coh}}$ of the cross correlation function is given by

$$C^{(1)}_{\mathrm{coh}}(\tau, \mathbf{x}_1, \mathbf{x}_2) = \int d\mathbf{y}\theta(\mathbf{y}) \int ds ds' F^\varepsilon(s') G_0(s, \mathbf{x}_1, \mathbf{y}) G_0(\tau + s + s', \mathbf{x}_2, \mathbf{y}),$$

where G_0 is the Green's function of the smoothly varying background.

2) The remaining coda component $C^{(1)}_{\mathrm{coda}}$, which is the contribution of the waves scattered by the inhomogeneities:

$$C^{(1)}_{\mathrm{coda}}(\tau, \mathbf{x}_1, \mathbf{x}_2) = C^{(1)}(\tau, \mathbf{x}_1, \mathbf{x}_2) - C^{(1)}_{\mathrm{coh}}(\tau, \mathbf{x}_1, \mathbf{x}_2). \tag{8.6}$$

We consider first the full fourth-order cross correlation function

$$C^{(2)}(\tau, \mathbf{x}_1, \mathbf{x}_2) = \lim_{T' \to \infty} \int_{-T'}^{T'} d\tau' \sum_j C^{(1)}(\tau', \mathbf{x}_{a,j}, \mathbf{x}_1) C^{(1)}(\tau' + \tau, \mathbf{x}_{a,j}, \mathbf{x}_2)$$

$$= \lim_{T' \to \infty} \int_{-T'}^{T'} d\tau' \int d\mathbf{x}_a \chi(\mathbf{x}_a) C^{(1)}(\tau', \mathbf{x}_a, \mathbf{x}_1) C^{(1)}(\tau' + \tau, \mathbf{x}_a, \mathbf{x}_2). \tag{8.7}$$

The following proposition is analogous to Proposition 5.1.

PROPOSITION 8.1. *To leading order the cross correlations $C^{(1)}(\tau, \mathbf{x}_1, \mathbf{x}_2)$ and $C^{(2)}(\tau, \mathbf{x}_1, \mathbf{x}_2)$ have singular components if and only if the ray going through $\mathbf{x}_1$ and $\mathbf{x}_2$ extends into the source region. If this is the case, then there are one or two singular components at $\tau = \pm\tau(\mathbf{x}_1, \mathbf{x}_2)$.*

Proof. The second-order cross correlation function $C^{(1)}$ is the sum of $C^{(1)}_{\mathrm{coh}}$ which has been analyzed in Proposition 5.1 and $C^{(1)}_{\mathrm{coda}}$ which is of order σ. We next consider the fourth-order cross correlation function. To leading order it is equal to

$$C^{(2)}(\tau, \mathbf{x}_1, \mathbf{x}_2) = \int d\mathbf{x}_a \chi(\mathbf{x}_a) \int d\tau' C^{(1)}_{\mathrm{coh}}(\tau', \mathbf{x}_a, \mathbf{x}) C^{(1)}_{\mathrm{coh}}(\tau' + \tau, \mathbf{x}_a, \mathbf{x}_2) + O(\sigma)$$

$$= \int d\mathbf{x}_a d\mathbf{y}_1 d\mathbf{y}_2 \chi(\mathbf{x}_a) \theta(\mathbf{y}_1) \theta(\mathbf{y}_2) \int d\tau' ds du s' du' F^\varepsilon(s') F^\varepsilon(u')$$

$$\times G_0(s, \mathbf{x}_a, \mathbf{y}_1) G_0(\tau' + s + s', \mathbf{x}_1, \mathbf{y}_1) G_0(u, \mathbf{x}_a, \mathbf{y}_2) G_0(\tau' + \tau + u + u', \mathbf{x}_2, \mathbf{y}_2).$$

In the Fourier domain it has the form

$$C^{(2)}(\tau, \mathbf{x}_1, \mathbf{x}_2) = \frac{1}{2\pi} \int d\mathbf{x}_\mathrm{a} d\mathbf{y}_1 d\mathbf{y}_2 \chi(\mathbf{x}_\mathrm{a}) \theta(\mathbf{y}_1) \theta(\mathbf{y}_2) \int d\omega \hat{F}^\varepsilon(\omega)^2 e^{-i\omega\tau}$$
$$\times \hat{G}_0(\omega, \mathbf{x}_\mathrm{a}, \mathbf{y}_1) \overline{\hat{G}_0}(\omega, \mathbf{x}_1, \mathbf{y}_1) \overline{\hat{G}_0}(\omega, \mathbf{x}_\mathrm{a}, \mathbf{y}_2) \hat{G}_0(\omega, \mathbf{x}_2, \mathbf{y}_2).$$

It is remarkable that all four Green's functions are evaluated at the same frequency, which comes from the fact that only cross correlation operations are involved. We analyze this expression in the high-frequency regime by using the WKB approximation (5.4) of $\hat{G}_0$. We find that $C^{(2)}$ has singular components (at $\tau = \pm\tau(\mathbf{x}_1, \mathbf{x}_2)$) only if we can find stationary phase configurations in which the source points $\mathbf{y}_1$, $\mathbf{y}_2$, the auxiliary sensor $\mathbf{x}_\mathrm{a}$ and the main sensors $\mathbf{x}_1$, $\mathbf{x}_2$ are along the same ray. In particular, there must be a ray starting inside the source region and going through $\mathbf{x}_1$ and $\mathbf{x}_2$, as in Proposition 5.1. $\qquad\qquad\qquad\qquad\qquad\qquad\qquad\qquad\qquad\qquad\qquad\square$

We see, therefore, that there is no gain in using the function $C^{(2)}$ in place of $C^{(1)}$ for travel time estimation when there is no scattering. However, when there is scattering there may be additional singular components in $C^{(1)}$ and in $C^{(2)}$ due to scattered waves, but they are small and buried in the contributions of the direct waves. The next subsection shows how to extract them.

8.4. Stationary phase analysis for coda (fourth-order) cross correlations. We now consider the coda cross correlation, as suggested by Campillo and Stehly, which is given by

$$C^{(3)}(\tau, \mathbf{x}_1, \mathbf{x}_2) = \lim_{T'\to\infty} \int_{-T'}^{T'} d\tau' \sum_j C_\mathrm{coda}^{(1)}(\tau', \mathbf{x}_{\mathrm{a},j}, \mathbf{x}_1) C_\mathrm{coda}^{(1)}(\tau' + \tau, \mathbf{x}_{\mathrm{a},j}, \mathbf{x}_2)$$

$$= \lim_{T'\to\infty} \int_{-T'}^{T'} d\tau' \int d\mathbf{x}_\mathrm{a} \chi(\mathbf{x}_\mathrm{a}) C_\mathrm{coda}^{(1)}(\tau', \mathbf{x}_\mathrm{a}, \mathbf{x}_1) C_\mathrm{coda}^{(1)}(\tau' + \tau, \mathbf{x}_\mathrm{a}, \mathbf{x}_2) \quad (8.8)$$

PROPOSITION 8.2. *There are two (and only two) high-frequency (singular) components in $C^{(3)}$, at times $\tau = \pm\tau(\mathbf{x}_1, \mathbf{x}_2)$, if the two following conditions hold:*
1) There are scatterers located along the ray going through $\mathbf{x}_1$ and $\mathbf{x}_2$, but not on the segment between $\mathbf{x}_1$ and $\mathbf{x}_2$. These scatterers are the basic ones for the enhanced travel time estimation.
2) There are auxiliary sensors located along rays going from the source region (the support of the function θ) to the basic scatterers (see Figure 8.2).

The important point here is that it is not required that the ray joining the sensors $\mathbf{x}_1$ and $\mathbf{x}_2$ extend into the source region as in Proposition 8.1. Therefore the configurations for which the coda cross correlation $C^{(3)}$ has a singular component at the travel time between $\mathbf{x}_1$ and $\mathbf{x}_2$ are much more general than the ones for which the standard cross correlation has a singular component.

Proposition 8.1 shows that the additional information about the travel time coming from the contributions of the scattered waves is buried in the standard cross correlation $C^{(1)}$ and in the full fourth-order cross correlation $C^{(2)}$, while Proposition 8.2 shows that this information appears to leading order in the coda (fourth-order) cross correlation $C^{(3)}$, because the contributions of the direct waves have been removed. Therefore, the coda cross correlation is the one that should be used. In other words, while the interesting singular component of the coda fourth-order cross correlation
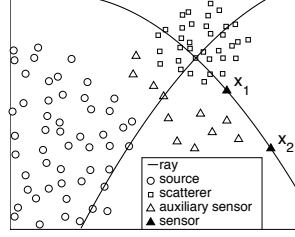
FIG. 8.2. *Schematic of a configuration of noise sources (circles), scatterers (squares), and auxiliary sensors (empty triangles) that give enhanced travel time estimation between* $\mathbf{x}_1$ *and* $\mathbf{x}_2$ *(solid triangles). First, there are scatterers along the ray going through* $\mathbf{x}_1$ *and* $\mathbf{x}_2$*. Second, there are auxiliary sensors along rays going from the source region into the scatterer region.*

is present in the full fourth-order cross correlation, it is buried in many other uninteresting (large) contributions, especially when the scattered waves are much weaker than the direct waves. That is why it is much better, in terms of the signal-to-noise ratio, to use the coda fourth-order cross correlations.

Proof. We consider the coda cross correlation $C^{(3)}$ in the form

$$
C^{(3)}(\tau, \mathbf{x}_1, \mathbf{x}_2) = \frac{1}{2\pi} \int d\mathbf{x}_{\mathrm{a}} d\mathbf{y}_1 d\mathbf{y}_2 \chi(\mathbf{x}_{\mathrm{a}})\theta(\mathbf{y}_1)\theta(\mathbf{y}_2) \int d\omega \hat{F}^{\varepsilon}(\omega)^2 e^{-i\omega\tau}
$$

$$
\times\Big(\hat{G}(\omega, \mathbf{x}_{\mathrm{a}}, \mathbf{y}_1)\overline{\hat{G}}(\omega, \mathbf{x}_1, \mathbf{y}_1) - \hat{G}_0(\omega, \mathbf{x}_{\mathrm{a}}, \mathbf{y}_1)\overline{\hat{G}_0}(\omega, \mathbf{x}_1, \mathbf{y}_1)\Big)
$$

$$
\times\Big(\overline{\hat{G}}(\omega, \mathbf{x}_{\mathrm{a}}, \mathbf{y}_2)\hat{G}(\omega, \mathbf{x}_2, \mathbf{y}_2) - \overline{\hat{G}_0}(\omega, \mathbf{x}_{\mathrm{a}}, \mathbf{y}_2)\hat{G}_0(\omega, \mathbf{x}_2, \mathbf{y}_2)\Big)
$$

$$
= \frac{1}{2\pi} \int d\mathbf{x}_{\mathrm{a}} d\mathbf{y}_1 d\mathbf{y}_2 \chi(\mathbf{x}_{\mathrm{a}})\theta(\mathbf{y}_1)\theta(\mathbf{y}_2) \int d\omega \hat{F}^{\varepsilon}(\omega)^2 e^{-i\omega\tau}
$$

$$
\times\Big(\hat{G}_0(\omega, \mathbf{x}_{\mathrm{a}}, \mathbf{y}_1)\overline{\hat{G}_1}(\omega, \mathbf{x}_1, \mathbf{y}_1) + \hat{G}_1(\omega, \mathbf{x}_{\mathrm{a}}, \mathbf{y}_1)\overline{\hat{G}_0}(\omega, \mathbf{x}_1, \mathbf{y}_1)\Big)
$$

$$
\times\Big(\overline{\hat{G}_0}(\omega, \mathbf{x}_{\mathrm{a}}, \mathbf{y}_2)\hat{G}_1(\omega, \mathbf{x}_2, \mathbf{y}_2) + \overline{\hat{G}_1}(\omega, \mathbf{x}_{\mathrm{a}}, \mathbf{y}_2)\hat{G}_0(\omega, \mathbf{x}_2, \mathbf{y}_2)\Big) + O(\sigma^3), \quad (8.9)
$$

where $\hat{G}_1$ is given by (8.3). We analyze the expectation $\mathbb{E}[C^{(3)}]$ with respect to the random medium. By keeping only the leading order terms there are four contributions to $\mathbb{E}[C^{(3)}]$:

$$
C_1^{(3)}(\tau, \mathbf{x}_1, \mathbf{x}_2) = \frac{\varepsilon\sigma^2}{2\pi} \int d\mathbf{x}_{\mathrm{a}} d\mathbf{y}_1 d\mathbf{y}_2 d\mathbf{z}_{\mathrm{s}} \chi(\mathbf{x}_{\mathrm{a}})\theta(\mathbf{y}_1)\theta(\mathbf{y}_2)\rho(\mathbf{z}_{\mathrm{s}}) \int d\omega\, \omega^4 \hat{F}(\omega)^2 e^{-i\frac{\omega}{\varepsilon}\tau}
$$

$$
\times\hat{G}_0\Big(\frac{\omega}{\varepsilon}, \mathbf{x}_{\mathrm{a}}, \mathbf{y}_1\Big)\overline{\hat{G}_0}\Big(\frac{\omega}{\varepsilon}, \mathbf{x}_1, \mathbf{z}_{\mathrm{s}}\Big)\overline{\hat{G}_0}\Big(\frac{\omega}{\varepsilon}, \mathbf{z}_{\mathrm{s}}, \mathbf{y}_1\Big)
$$

$$
\times\overline{\hat{G}_0}\Big(\frac{\omega}{\varepsilon}, \mathbf{x}_{\mathrm{a}}, \mathbf{y}_2\Big)\hat{G}_0\Big(\frac{\omega}{\varepsilon}, \mathbf{x}_2, \mathbf{z}_{\mathrm{s}}\Big)\hat{G}_0\Big(\frac{\omega}{\varepsilon}, \mathbf{z}_{\mathrm{s}}, \mathbf{y}_2\Big),
$$

$$
C_2^{(3)}(\tau, \mathbf{x}_1, \mathbf{x}_2) = \frac{\varepsilon\sigma^2}{2\pi} \int d\mathbf{x}_{\mathrm{a}} d\mathbf{y}_1 d\mathbf{y}_2 d\mathbf{z}_{\mathrm{s}} \chi(\mathbf{x}_{\mathrm{a}})\theta(\mathbf{y}_1)\theta(\mathbf{y}_2)\rho(\mathbf{z}_{\mathrm{s}}) \int d\omega\, \omega^4 \hat{F}(\omega)^2 e^{-i\frac{\omega}{\varepsilon}\tau}
$$

$$
\times\hat{G}_0\Big(\frac{\omega}{\varepsilon}, \mathbf{x}_{\mathrm{a}}, \mathbf{z}_{\mathrm{s}}\Big)\hat{G}_0\Big(\frac{\omega}{\varepsilon}, \mathbf{z}_{\mathrm{s}}, \mathbf{y}_1\Big)\overline{\hat{G}_0}\Big(\frac{\omega}{\varepsilon}, \mathbf{x}_1, \mathbf{y}_1\Big)
$$

$$
\times\overline{\hat{G}_0}\Big(\frac{\omega}{\varepsilon}, \mathbf{x}_{\mathrm{a}}, \mathbf{y}_2\Big)\hat{G}_0\Big(\frac{\omega}{\varepsilon}, \mathbf{x}_2, \mathbf{z}_{\mathrm{s}}\Big)\hat{G}_0\Big(\frac{\omega}{\varepsilon}, \mathbf{z}_{\mathrm{s}}, \mathbf{y}_2\Big),
$$

$$C_3^{(3)}(\tau, \mathbf{x}_1, \mathbf{x}_2) = \frac{\varepsilon \sigma^2}{2\pi} \int d\mathbf{x}_a dy_1 dy_2 d\mathbf{z}_s \chi(\mathbf{x}_a)\theta(\mathbf{y}_1)\theta(\mathbf{y}_2)\rho(\mathbf{z}_s) \int d\omega\, \omega^4 \hat{F}(\omega)^2 e^{-i\frac{\omega}{\varepsilon}\tau}$$

$$\times \hat{G}_0\left(\frac{\omega}{\varepsilon}, \mathbf{x}_a, \mathbf{y}_1\right) \overline{\hat{G}_0}\left(\frac{\omega}{\varepsilon}, \mathbf{x}_1, \mathbf{z}_s\right) \overline{\hat{G}_0}\left(\frac{\omega}{\varepsilon}, \mathbf{z}_s, \mathbf{y}_1\right)$$

$$\times \overline{\hat{G}_0}\left(\frac{\omega}{\varepsilon}, \mathbf{x}_a, \mathbf{z}_s\right) \hat{G}_0\left(\frac{\omega}{\varepsilon}, \mathbf{z}_s, \mathbf{y}_2\right) \hat{G}_0\left(\frac{\omega}{\varepsilon}, \mathbf{x}_2, \mathbf{y}_2\right),$$

$$C_4^{(3)}(\tau, \mathbf{x}_1, \mathbf{x}_2) = \frac{\varepsilon \sigma^2}{2\pi} \int d\mathbf{x}_a dy_1 dy_2 d\mathbf{z}_s \chi(\mathbf{x}_a)\theta(\mathbf{y}_1)\theta(\mathbf{y}_2)\rho(\mathbf{z}_s) \int d\omega\, \omega^4 \hat{F}(\omega)^2 e^{-i\frac{\omega}{\varepsilon}\tau}$$

$$\times \hat{G}_0\left(\frac{\omega}{\varepsilon}, \mathbf{x}_a, \mathbf{z}_s\right) \hat{G}_0\left(\frac{\omega}{\varepsilon}, \mathbf{z}_s, \mathbf{y}_1\right) \overline{\hat{G}_0}\left(\frac{\omega}{\varepsilon}, \mathbf{x}_1, \mathbf{y}_1\right)$$

$$\times \overline{\hat{G}_0}\left(\frac{\omega}{\varepsilon}, \mathbf{x}_a, \mathbf{z}_s\right) \overline{\hat{G}_0}\left(\frac{\omega}{\varepsilon}, \mathbf{z}_s, \mathbf{y}_2\right) \hat{G}_0\left(\frac{\omega}{\varepsilon}, \mathbf{x}_2, \mathbf{y}_2\right).$$

We will analyze each of these four contributions in the high-frequency regime using the stationary phase method.

We consider the first contribution $C_1^{(3)}$. Using the WKB approximation (5.4) of the background Green's function, we obtain:

$$C_1^{(3)}(\tau, \mathbf{x}_1, \mathbf{x}_2) = \frac{\varepsilon \sigma^2}{2\pi} \int d\mathbf{x}_a dy_1 dy_2 d\mathbf{z}_s \chi(\mathbf{x}_a)\theta(\mathbf{y}_1)\theta(\mathbf{y}_2)\rho(\mathbf{z}_s) \int d\omega\, \omega^4 \hat{F}(\omega)^2$$

$$\times a(\mathbf{x}_a, \mathbf{y}_1)\overline{a}(\mathbf{x}_1, \mathbf{z}_s)\overline{a}(\mathbf{z}_s, \mathbf{y}_1)\overline{a}(\mathbf{x}_a, \mathbf{y}_2)a(\mathbf{x}_2, \mathbf{z}_s)a(\mathbf{z}_s, \mathbf{y}_2)e^{i\frac{\omega}{\varepsilon}\mathcal{T}(\mathbf{x}_a, \mathbf{y}_1, \mathbf{y}_2, \mathbf{z}_s)}.$$

The rapid phase is

$$\omega\mathcal{T}(\mathbf{x}_a, \mathbf{y}_1, \mathbf{y}_2, \mathbf{z}_s) = \omega\big[\tau(\mathbf{x}_a, \mathbf{y}_1) - \tau(\mathbf{x}_1, \mathbf{z}_s) - \tau(\mathbf{z}_s, \mathbf{y}_1)$$
$$-\tau(\mathbf{x}_a, \mathbf{y}_2) + \tau(\mathbf{x}_2, \mathbf{z}_s) + \tau(\mathbf{z}_s, \mathbf{y}_2) - \tau\big].$$

The dominant contribution comes from the stationary phase points satisfying

$$\big(\partial_\omega, \nabla_{\mathbf{x}_a}, \nabla_{\mathbf{y}_1}, \nabla_{\mathbf{y}_2}, \nabla_{\mathbf{z}_s}\big)\big(\omega\mathcal{T}(\mathbf{x}_a, \mathbf{y}_1, \mathbf{y}_2, \mathbf{z}_s)\big) = \big(0, \mathbf{0}, \mathbf{0}, \mathbf{0}, \mathbf{0}\big),$$

which give the five conditions

$$\tau(\mathbf{x}_a, \mathbf{y}_1) - \tau(\mathbf{x}_1, \mathbf{z}_s) - \tau(\mathbf{z}_s, \mathbf{y}_1) - \tau(\mathbf{x}_a, \mathbf{y}_2) + \tau(\mathbf{x}_2, \mathbf{z}_s) + \tau(\mathbf{z}_s, \mathbf{y}_2) = \tau,$$
$$\nabla_{\mathbf{x}_a}\tau(\mathbf{x}_a, \mathbf{y}_1) = \nabla_{\mathbf{x}_a}\tau(\mathbf{x}_a, \mathbf{y}_2),$$
$$\nabla_{\mathbf{y}_1}\tau(\mathbf{y}_1, \mathbf{x}_a) = \nabla_{\mathbf{y}_1}\tau(\mathbf{y}_1, \mathbf{z}_s),$$
$$\nabla_{\mathbf{y}_2}\tau(\mathbf{y}_2, \mathbf{x}_a) = \nabla_{\mathbf{y}_2}\tau(\mathbf{y}_2, \mathbf{z}_s),$$
$$\nabla_{\mathbf{z}_s}\tau(\mathbf{z}_s, \mathbf{x}_1) + \nabla_{\mathbf{z}_s}\tau(\mathbf{z}_s, \mathbf{y}_1) = \nabla_{\mathbf{z}_s}\tau(\mathbf{z}_s, \mathbf{x}_2) + \nabla_{\mathbf{z}_s}\tau(\mathbf{z}_s, \mathbf{y}_2).$$

It turns out that there do exist such stationary points for $C_1^{(3)}$. They are determined by using Lemma B.1. The second condition means that $\mathbf{y}_1$ and $\mathbf{y}_2$ lie on the same side of a ray issuing from $\mathbf{x}_a$. The third one means that $\mathbf{x}_a$ and $\mathbf{z}_s$ lie on the same side of a ray issuing from $\mathbf{y}_1$. Therefore, $\mathbf{y}_1$, $\mathbf{y}_2$, $\mathbf{z}_s$ and $\mathbf{x}_a$ are on the same ray, with the pairs $(\mathbf{y}_1, \mathbf{y}_2)$ and $(\mathbf{z}_s, \mathbf{x}_a)$ on opposite sides. There are four possibilities: $\mathbf{y}_1 \to \mathbf{y}_2 \to \mathbf{z}_s \to \mathbf{x}_a$, $\mathbf{y}_2 \to \mathbf{y}_1 \to \mathbf{z}_s \to \mathbf{x}_a$, $\mathbf{y}_1 \to \mathbf{y}_2 \to \mathbf{x}_a \to \mathbf{z}_s$, and $\mathbf{y}_2 \to \mathbf{y}_1 \to \mathbf{x}_a \to \mathbf{z}_s$.

The fourth condition is now automatically satisfied and the last condition can be simplified to $\nabla_{\mathbf{z}_s}\tau(\mathbf{z}_s, \mathbf{x}_1) = \nabla_{\mathbf{z}_s}\tau(\mathbf{z}_s, \mathbf{x}_2)$, which means that $\mathbf{x}_1$ and $\mathbf{x}_2$ are on the same side of a ray issuing from $\mathbf{z}_s$. There are two possibilities here: $\mathbf{z}_s \to \mathbf{x}_1 \to \mathbf{x}_2$

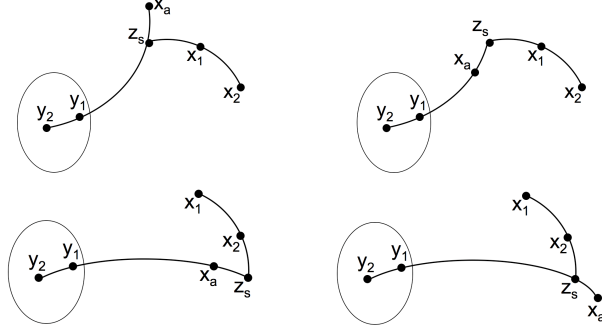FIG. 8.3. *Four contributions to the stationary phase of* $C_1^{(3)}$ *when the support of the noise sources is the ellipse shown and* $\mathbf{y}_1$ *and* $\mathbf{y}_2$ *are two points in it. The main sensors are at* $\mathbf{x}_1$ *and* $\mathbf{x}_2$. *An auxiliary sensor is at* $\mathbf{x}_a$ *and a scatterer at* $\mathbf{z}_s$. *The points* $\mathbf{y}_1, \mathbf{y}_2, \mathbf{z}_s, \mathbf{x}_a$ *are along the same ray, as are* $\mathbf{z}_s, \mathbf{x}_1, \mathbf{x}_2$. *The two configurations on the top contribute at* $\tau = \tau(\mathbf{x}_1, \mathbf{x}_2)$. *The two configurations on the bottom contribute at* $\tau = -\tau(\mathbf{x}_1, \mathbf{x}_2)$. *The other four configurations are obtained by interchanging* $\mathbf{y}_1$ *and* $\mathbf{y}_2$.

and $\mathbf{z}_s \to \mathbf{x}_2 \to \mathbf{x}_1$. Consequently, there are eight types of configurations of points satisfying the last four conditions (Figure 8.3). They all contribute to the term $C_1^{(3)}$ if in addition the first condition is satisfied, which is simply $\tau = \tau(\mathbf{x}_1, \mathbf{x}_2)$ if $\mathbf{x}_1$ is between $\mathbf{z}_s$ and $\mathbf{x}_2$, and $\tau = -\tau(\mathbf{x}_1, \mathbf{x}_2)$ if $\mathbf{x}_2$ is between $\mathbf{z}_s$ and $\mathbf{x}_1$. Therefore, there are only two singular components in $C_1^{(3)}$, which are at times $\tau = \pm\tau(\mathbf{x}_1, \mathbf{x}_2)$. By considering the Hessian of $\omega\mathcal{T}$ (with respect to ω, $\mathbf{x}_a$, $\mathbf{y}_1$, $\mathbf{y}_2$, $\mathbf{z}_s$) we find by the stationary phase theorem that the amplitudes of the contributions of these stationary maps to $\mathbb{E}[C_3]$ are of order $\sigma^2\varepsilon^{1+3(d-1)/2}$ (this will be used below).

We examine next the three other terms $C_j^{(3)}$, $j = 2, 3, 4$. They also have stationary points that give peaks at times $\tau = \pm\tau(\mathbf{x}_1, \mathbf{x}_2)$, but only in configurations for which a source point ($\mathbf{y}_1$ or $\mathbf{y}_2$), a scatterer point ($\mathbf{z}_s$) and the two sensors $\mathbf{x}_1$ and $\mathbf{x}_2$ are along the same ray, while the other source point, the scatterer $\mathbf{z}_s$ and the auxiliary sensor $\mathbf{x}_a$ are along another ray. In particular, a source and the sensors $\mathbf{x}_1$ and $\mathbf{x}_2$ must be on the same ray. If this is the case the stationary phase approximation gives amplitudes of the order of $\sigma^2\varepsilon^{1+3(d-1)/2}$.

To complete the proof we need to show that the fluctuations of $C^{(3)}$ due to the random medium are small. The calculations carried out for the expectation $\mathbb{E}[C^{(3)}]$ give then correct results for $C^{(3)}$ itself. We analyze the variance $\mathrm{Var}(C^{(3)}) = \mathbb{E}[(C^{(3)})^2] - \mathbb{E}[C^{(3)}]^2$ and show that it is much smaller than $\mathbb{E}[C^{(3)}]^2$. Using (8.9), the property (8.5), and the standard rule for the calculations of fourth-order moments of Gaussian processes, we find that the leading order term of the variance is of order σ^4 and consists of 32 contributions (there are 48 contributions for $\mathbb{E}[(C^{(3)})^2]$, and among

them 16 are canceled by $\mathbb{E}[C^{(3)}]^2)$. One of these contributions is

$$
\begin{aligned}
V_{41}^{(3)} = \frac{\sigma^4 \varepsilon^2}{4\pi^2} &\int d\mathbf{x}_\mathrm{a} d\mathbf{y}_1 d\mathbf{y}_2 d\mathbf{z}_\mathrm{s} \chi(\mathbf{x}_\mathrm{a}) \theta(\mathbf{y}_1) \theta(\mathbf{y}_2) \rho(\mathbf{z}_\mathrm{s}) \int d\omega\, \omega^4 \hat{F}(\omega)^2 e^{-i\frac{\omega}{\varepsilon}\tau} \\
&\times \int d\mathbf{x}'_\mathrm{a} d\mathbf{y}'_1 d\mathbf{y}'_2 d\mathbf{z}'_\mathrm{s} \chi(\mathbf{x}'_\mathrm{a}) \theta(\mathbf{y}'_1) \theta(\mathbf{y}'_2) \rho(\mathbf{z}'_\mathrm{s}) \int d\omega'\, \omega'^4 \hat{F}(\omega')^2 e^{i\frac{\omega'}{\varepsilon}\tau} \\
&\times \hat{G}_0\Big(\frac{\omega}{\varepsilon}, \mathbf{x}_\mathrm{a}, \mathbf{y}_1\Big) \overline{\hat{G}_0}\Big(\frac{\omega}{\varepsilon}, \mathbf{x}_1, \mathbf{z}_\mathrm{s}\Big) \overline{\hat{G}_0}\Big(\frac{\omega}{\varepsilon}, \mathbf{z}_\mathrm{s}, \mathbf{y}_1\Big) \\
&\times \overline{\hat{G}_0}\Big(\frac{\omega}{\varepsilon}, \mathbf{x}_\mathrm{a}, \mathbf{y}_2\Big) \hat{G}_0\Big(\frac{\omega}{\varepsilon}, \mathbf{x}_2, \mathbf{z}'_\mathrm{s}\Big) \hat{G}_0\Big(\frac{\omega}{\varepsilon}, \mathbf{z}'_\mathrm{s}, \mathbf{y}_2\Big) \\
&\times \overline{\hat{G}_0}\Big(\frac{\omega'}{\varepsilon}, \mathbf{x}'_\mathrm{a}, \mathbf{y}'_1\Big) \hat{G}_0\Big(\frac{\omega'}{\varepsilon}, \mathbf{x}_1, \mathbf{z}'_\mathrm{s}\Big) \hat{G}_0\Big(\frac{\omega'}{\varepsilon}, \mathbf{z}'_\mathrm{s}, \mathbf{y}'_1\Big) \\
&\times \hat{G}_0\Big(\frac{\omega'}{\varepsilon}, \mathbf{x}'_\mathrm{a}, \mathbf{y}'_2\Big) \overline{\hat{G}_0}\Big(\frac{\omega'}{\varepsilon}, \mathbf{x}_2, \mathbf{z}_\mathrm{s}\Big) \overline{\hat{G}_0}\Big(\frac{\omega'}{\varepsilon}, \mathbf{z}_\mathrm{s}, \mathbf{y}'_2\Big).
\end{aligned}
$$

Using the WKB approximation of the background Green's function, we obtain an expression in which the rapid phase is

$$
\begin{aligned}
\phi = \omega\big[&\tau(\mathbf{x}_\mathrm{a}, \mathbf{y}_1) - \tau(\mathbf{x}_1, \mathbf{z}_\mathrm{s}) - \tau(\mathbf{z}_\mathrm{s}, \mathbf{y}_1) - \tau(\mathbf{x}_\mathrm{a}, \mathbf{y}_2) + \tau(\mathbf{x}_2, \mathbf{z}'_\mathrm{s}) + \tau(\mathbf{z}'_\mathrm{s}, \mathbf{y}_2) - \tau\big] \\
-\omega'\big[&\tau(\mathbf{x}'_\mathrm{a}, \mathbf{y}'_1) - \tau(\mathbf{x}_1, \mathbf{z}'_\mathrm{s}) - \tau(\mathbf{z}'_\mathrm{s}, \mathbf{y}'_1) - \tau(\mathbf{x}'_\mathrm{a}, \mathbf{y}'_2) + \tau(\mathbf{x}_2, \mathbf{z}_\mathrm{s}) + \tau(\mathbf{z}_\mathrm{s}, \mathbf{y}'_2) + \tau\big].
\end{aligned}
$$

Stationary points for this exist only if all points are along the same ray. Consequently it is necessary that the ray going through $\mathbf{x}_1$ and $\mathbf{x}_2$ reach into the source region, and then the amplitudes of the contributions of these stationary maps given by the stationary phase theorem are of the order of $\sigma^4 \varepsilon^{2+8(d-1)/2}$. This is much smaller than $\sigma^4 \varepsilon^{2+6(d-1)/2}$, which is the order of magnitude of the main contributions to the square of $\mathbb{E}[C^{(3)}]$. The other 31 components of the variance of $C^{(3)}$ behave similarly, and some have even smaller contributions. This shows that the fluctuations of $C^{(3)}$ due to the random medium are small when we consider singular components. $\qquad\square$

8.5. Statistical stability of fourth-order cross correlation functions. For completeness, we analyze also the role that the fluctuations $C_T - \langle C_T \rangle$, due to the noise sources, play in fourth-order cross correlations. We show that, as may be expected, they are negligible. More precisely, we consider the fluctuations of the cross correlation

$$
\widetilde{C}_T(\tau, \mathbf{x}_1, \mathbf{x}_2) = C_T(\tau, \mathbf{x}_1, \mathbf{x}_2) - \langle C_T(\tau, \mathbf{x}_1, \mathbf{x}_2) \rangle , \tag{8.10}
$$

we compute the cross correlations between $(\mathbf{x}_1, \mathbf{x}_{\mathrm{a},j})$ and $(\mathbf{x}_2, \mathbf{x}_{\mathrm{a},j})$, for all auxiliary sensors $\mathbf{x}_{\mathrm{a},j}$, and we study the cross correlation of the fluctuations

$$
\begin{aligned}
\widetilde{C}^{(2)}_{T',T}(\tau, \mathbf{x}_1, \mathbf{x}_2) &= \int_{-T'}^{T'} d\tau' \sum_j \widetilde{C}_T(\tau', \mathbf{x}_{\mathrm{a},j}, \mathbf{x}_1) \widetilde{C}_T(\tau' + \tau, \mathbf{x}_{\mathrm{a},j}, \mathbf{x}_2) \\
&= \int_{-T'}^{T'} d\tau' \int d\mathbf{x}_\mathrm{a} \chi(\mathbf{x}_\mathrm{a}) \widetilde{C}_T(\tau', \mathbf{x}_\mathrm{a}, \mathbf{x}_1) \widetilde{C}_T(\tau' + \tau, \mathbf{x}_\mathrm{a}, \mathbf{x}_2). \tag{8.11}
\end{aligned}
$$

PROPOSITION 8.3. *The cross correlation fluctuations $\widetilde{C}^{(2)}_{T',T}(\tau, \mathbf{x}_1, \mathbf{x}_2)$ converge to zero in probability as $T, T' \to \infty$.*
More precisely, $T\widetilde{C}^{(2)}_{T',T}(\tau, \mathbf{x}_1, \mathbf{x}_2)$ is self-averaging as $T, T' \to \infty$:

$$
T\widetilde{C}^{(2)}_{T',T}(\tau, \mathbf{x}_1, \mathbf{x}_2) \overset{T,T'\to\infty}{\longrightarrow} \widetilde{C}^{(2)}(\tau, \mathbf{x}_1, \mathbf{x}_2).
$$

The normalized cross correlation $\widetilde{C}^{(2)}(\tau, \mathbf{x}_1, \mathbf{x}_2)$ has a singular component if and only if the ray going through $\mathbf{x}_1$ and $\mathbf{x}_2$ reaches into the source region. There are then one or two singular components at $\tau = \pm\tau(\mathbf{x}_1, \mathbf{x}_2)$.

   This proposition shows that the fluctuations in the fourth-order cross correlations due to the noise sources decay to zero as T^{-1}. Propositions 5.1 and 8.3 show also that $\widetilde{C}^{(2)}(\tau, \mathbf{x}_1, \mathbf{x}_2)$ and $C^{(1)}(\tau, \mathbf{x}_1, \mathbf{x}_2)$ carry the same information in their singular components. In other words, the small fluctuations of the cross correlations due to the noise sources have no new information regarding travel times. As shown by Proposition 8.2, it is the tails (or coda) of the cross correlations generated by the inhomogeneities of the medium that contain buried information about travel times, and this information can be extracted by computing the $C^{(3)}$ cross correlation.

   8.6. Higher-order cross correlations. We have considered an inhomogeneous medium with weak, randomly distributed point scatterers. Waves scattered by point scatterers are spherical and have no directional memory of the incident waves. This complete isotropization of the scattered field is desirable in order to have good reconstruction of the Green's function from coda cross correlations. However, enhanced travel time estimation using iterated cross correlations can occur in other scattering media as well. It may be necessary to use higher-order cross correlations in media in which scattering is not isotropic, as we now explain.

   A possible way to use higher-order cross-correlations is to iterate further coda cross correlations as follows:

1) Compute the cross correlation between all pairs of sensors, including between pairs of auxiliary sensors.

2) Cross correlate the coda of the cross correlations in order get fourth-order cross correlation functions:

$$C_{T,T'}(\tau, \mathbf{x}_j, \mathbf{x}_{\mathrm{a},l}) = \sum_{k=1}^{N} \int_{[-T',-T_{\mathrm{coda}}]\cup[T_{\mathrm{coda}},T']} C_T(\tau', \mathbf{x}_{\mathrm{a},k}, \mathbf{x}_j) C_T(\tau' + \tau, \mathbf{x}_{\mathrm{a},k}, \mathbf{x}_{\mathrm{a},l}) d\tau',$$

for $j = 1, 2$ and for all auxiliary sensors at $\mathbf{x}_{\mathrm{a},l}$, $l = 1, \ldots, N$.

3) Cross correlate the coda of the fourth-order cross correlation functions in order to get the eighth-order cross correlation function:

$$C_{T,T',T''}(\tau, \mathbf{x}_1, \mathbf{x}_2) = \sum_{l=1}^{N} \int_{[-T'',-T_{\mathrm{coda}}]\cup[T_{\mathrm{coda}},T'']} C_{T,T'}(\tau', \mathbf{x}_1, \mathbf{x}_{\mathrm{a},l})$$
$$\times C_{T,T'}(\tau' + \tau, \mathbf{x}_2, \mathbf{x}_{\mathrm{a},l}) d\tau'.$$

The coda cross correlation $C_{T,T'}(\tau, \mathbf{x}_1, \mathbf{x}_2)$ proposed by Campillo and Stehly and studied in this paper removes contributions of the direct waves and exploits the scattered waves. Higher-order cross correlations, such as $C_{T,T',T''}(\tau, \mathbf{x}_1, \mathbf{x}_2)$ remove contributions of direct waves and of those of single-scattered waves. They exploit mainly multiply-scattered waves. When single scattering is not isotropic then multiply scattered waves tend to be more isotropic than direct and single-scattered waves. When single scattering is essentially isotropic then it is unlikely that higher-order cross correlations will give better results than coda cross correlations. A more quantitative analysis, including signal-to-noise ratios, is needed in order to substantiate these comments.

   9. Summary and conclusions. We have presented and analyzed an integrated framework for reflector imaging and travel time estimation with *passive sensor networks*, using cross correlations of signals generated by ambient noise sources.

We have shown in Sections 6-7 that imaging of reflectors by migrating cross correlations can be effective carried out if the migration travel times are chosen appropriately, depending on the positions of the reflectors to be imaged relative to the sensors and the noise sources. More precisely:

1) For daylight configurations (Subsection 6.3), we have shown that the imaging functional is similar to Kirchhoff or travel time migration for passive reflectors illuminated by active sensors. It is, therefore, possible to assess resolution rather well in daylight illumination configurations. In particular, the range resolution is inversely proportional to the bandwidth and the cross range resolution is proportional to the Rayleigh resolution formula for sensor arrays (Subsection 6.4). We can also consider optimal illumination in the cross correlation context following the ideas proposed in [8, 9] in the active array context. This means that weights could be introduced in the daylight imaging functional to compensate for possible imbalances between the illuminations received by the different sensors from the ambient noise sources.

2) In backlight configurations (Subsection 6.5), we have shown that the imaging functional is similar to Kirchhoff migration for imaging active noise sources recorded by passive sensors. Because of this analogy, we know that range resolution is very poor and that only the direction of arrival can be estimated with sensor arrays.

3) We have shown (Subsection 7.2) how coherent interferometric imaging (CINT) can be implemented when there is scattering in the medium.

We have also analyzed travel time estimation by cross correlation of noisy signals. We have shown analytically how directionality of the energy flux from the noise sources affects the quality of the travel time estimates. We have shown how iterated cross correlations with auxiliary sensors in a scattering medium can enhance the quality of the travel time estimates. In Section 8 we have given an analytical justification of the fourth-order cross correlation technique proposed by Campillo and Stehly [13]. We have identified configurations of scatterers and the auxiliary sensor locations that play a significant role in this enhancement:

1) Scatterers that are along the ray joining the principal sensors.

2) Auxiliary sensors that are along rays connecting source points and scatterers identified in 1).

As noted in the introduction, most applications of cross correlation techniques with passive sensor data are, so far, in geophysics. They may, however, be useful in other contexts, in microwave regimes in particular. Wireless cell phones in an urban environment, or in an indoor environment, could be considered as statistically stationary, spatially distributed noise sources. At a central frequency of 2.4 GHz (12 centimeter wavelength) and a bandwidth of 20 MHz the expected travel time resolution is about 10 meters. With a 200 MHz bandwidth the expected resolution is about 1 meter. Exploiting multiple scattering could make possible the use of passive microwave sensor networks to monitor changes in the environment with differential cross correlations. This would have the advantage of being both passive and rather sensitive but will likely require additional information about the environment, such as indoor floor plans or the location of buildings in an urban setting. A detailed analysis, taking into account the relatively small bandwidth and the scattering properties of microwaves in such environments, is currently under study.

Appendix A. Proof of Proposition 4.1. In this appendix we prove Proposition 4.1. It establishes statistical stability of the cross correlations with respect to noise source fluctuations.

By the stationarity of the process n^ε, the product $u(t, \mathbf{x}_1)u(t + \tau, \mathbf{x}_2)$ is itself a stationary random process in t. Therefore the mean of C_T is independent of T and is given by

$$\langle C_T(\tau, \mathbf{x}_1, \mathbf{x}_2)\rangle = \langle u(0, \mathbf{x}_1)u(\tau, \mathbf{x}_2)\rangle .$$

Using (4.7) we get the following integral representation for the average of the cross correlation function:

$$\langle C_T(\tau, \mathbf{x}_1, \mathbf{x}_2)\rangle = \int d\mathbf{y}_1 d\mathbf{y}_2 \int ds' ds\, G(s, \mathbf{x}_1, \mathbf{y}_1)G(s', \mathbf{x}_2, \mathbf{y}_2)$$
$$\times \langle n^\varepsilon(-s, \mathbf{y}_1)n^\varepsilon(\tau - s', \mathbf{y}_2)\rangle .$$

Using the form (4.2) of the autocorrelation function of the sources, we obtain

$$\langle C_T(\tau, \mathbf{x}_1, \mathbf{x}_2)\rangle = \int d\mathbf{y}_1 d\mathbf{y}_2 \int ds' ds\, G(s, \mathbf{x}_1, \mathbf{y}_1)G(\tau + s + s', \mathbf{x}_2, \mathbf{y}_2)F^\varepsilon(s')\Gamma(\mathbf{y}_1, \mathbf{y}_2) .$$

Using the spatial delta-correlation property (4.6) we obtain (4.11), which in the Fourier domain is (4.12).

In order to prove the self-averaging property of the cross correlation function C_T we compute its variance. The principle of this computation is the following one. We first write the covariance function of C_T as a multiple integral which involves the fourth-order moment of the random process n^ε. Since n^ε is Gaussian, this fourth-order moment can be written as the sum of products of second-order moments, which makes the computation tractable. Using (4.7) and (4.9), the complete expression of the covariance function is

$$\mathrm{Cov}\big(C_T(\tau, \mathbf{x}_1, \mathbf{x}_2), C_T(\tau + \Delta\tau, \mathbf{x}_1, \mathbf{x}_2)\big) =$$
$$\frac{1}{T^2}\int_0^T\int_0^T dt dt' \int ds ds' du du' \int d\mathbf{y}_1 d\mathbf{y}_1' d\mathbf{y}_2 d\mathbf{y}_2'$$
$$\times G(s, \mathbf{x}_1, \mathbf{y}_1)G(u - \tau, \mathbf{x}_1, \mathbf{y}_2)G(s', \mathbf{x}_2, \mathbf{y}_1')G(u' - \tau - \Delta\tau, \mathbf{x}_2, \mathbf{y}_2')$$
$$\times \Big(\langle n^\varepsilon(t - s, \mathbf{y}_1)n^\varepsilon(t - u, \mathbf{y}_2)n^\varepsilon(t' - s', \mathbf{y}_1')n^\varepsilon(t' - u', \mathbf{y}_2')\rangle$$
$$- \langle n^\varepsilon(t - s, \mathbf{y}_1)n^\varepsilon(t - u, \mathbf{y}_2)\rangle\, \langle n^\varepsilon(t' - s', \mathbf{y}_1')n^\varepsilon(t' - u', \mathbf{y}_2')\rangle \Big) . \qquad \text{(A.1)}$$

The product of second-order moments of the random process n^ε is

$$\langle n^\varepsilon(t - s, \mathbf{y}_1)n^\varepsilon(t - u, \mathbf{y}_2)\rangle\, \langle n^\varepsilon(t' - s', \mathbf{y}_1')n^\varepsilon(t' - u', \mathbf{y}_2')\rangle$$
$$= F^\varepsilon(s - u)F^\varepsilon(s' - u')\theta(\mathbf{y}_1)\delta(\mathbf{y}_1 - \mathbf{y}_2)\theta(\mathbf{y}_1')\delta(\mathbf{y}_1' - \mathbf{y}_2') .$$

The fourth-order moment of the Gaussian random process n^ε is

$$\langle n^\varepsilon(t - s, \mathbf{y}_1)n^\varepsilon(t - u, \mathbf{y}_2)n^\varepsilon(t' - s', \mathbf{y}_1')n^\varepsilon(t' - u', \mathbf{y}_2')\rangle$$
$$= F^\varepsilon(s - u)F^\varepsilon(s' - u')\theta(\mathbf{y}_1)\delta(\mathbf{y}_1 - \mathbf{y}_2)\theta(\mathbf{y}_1')\delta(\mathbf{y}_1' - \mathbf{y}_2')$$
$$+ F^\varepsilon(t - t' - s + s')F^\varepsilon(t - t' - u + u')\theta(\mathbf{y}_1)\delta(\mathbf{y}_1 - \mathbf{y}_1')\theta(\mathbf{y}_2)\delta(\mathbf{y}_2 - \mathbf{y}_2')$$
$$+ F^\varepsilon(t - t' - s + u')F^\varepsilon(t - t' - u + s')\theta(\mathbf{y}_1)\delta(\mathbf{y}_1 - \mathbf{y}_2')\theta(\mathbf{y}_2)\delta(\mathbf{y}_1' - \mathbf{y}_2) .$$

Consequently, we have that for any $T > 0$

$$\frac{1}{T^2} \int_0^T \int_0^T dt dt' \Big(\langle n^\varepsilon(t-s, \mathbf{y}_1) n^\varepsilon(t-u, \mathbf{y}_2) n^\varepsilon(t'-s', \mathbf{y}_1') n^\varepsilon(t'-u', \mathbf{y}_2') \rangle$$

$$- \langle n^\varepsilon(t-s, \mathbf{y}_1) n^\varepsilon(t-u, \mathbf{y}_2) \rangle \langle n^\varepsilon(t'-s', \mathbf{y}_1') n^\varepsilon(t'-u', \mathbf{y}_2') \rangle \Big)$$

$$= S_T^\varepsilon(s'-s, u'-u) \theta(\mathbf{y}_1) \delta(\mathbf{y}_1 - \mathbf{y}_1') \theta(\mathbf{y}_2) \delta(\mathbf{y}_2 - \mathbf{y}_2')$$
$$+ S_T^\varepsilon(u'-s, s'-u) \theta(\mathbf{y}_1) \delta(\mathbf{y}_1 - \mathbf{y}_2') \theta(\mathbf{y}_2) \delta(\mathbf{y}_1' - \mathbf{y}_2), \qquad (A.2)$$

where

$$S_T^\varepsilon(s, u) = \frac{1}{4\pi^2} \int\int d\omega d\omega' \hat{F}^\varepsilon(\omega) \hat{F}^\varepsilon(\omega') \mathrm{sinc}^2\Big(\frac{(\omega - \omega')T}{2}\Big) e^{i\omega s - i\omega' u}.$$

Substituting into (A.1), we obtain for all $T > 0$ the following expression for the covariance function:

$$\mathrm{Cov}\big(C_T(\tau, \mathbf{x}_1, \mathbf{x}_2), C_T(\tau + \Delta\tau, \mathbf{x}_1, \mathbf{x}_2)\big) =$$
$$\frac{1}{4\pi^2} \int d\mathbf{x}_0 d\mathbf{y}_0 \theta(\mathbf{y}_1) \theta(\mathbf{y}_2) \int d\omega d\omega' \hat{F}^\varepsilon(\omega) \hat{F}^\varepsilon(\omega') e^{i\omega'\Delta\tau}$$

$$\times \overline{\hat{G}}(\omega, \mathbf{x}_1, \mathbf{y}_1) \hat{G}(\omega, \mathbf{x}_2, \mathbf{y}_1) \hat{G}(\omega', \mathbf{x}_1, \mathbf{y}_2) \overline{\hat{G}}(\omega', \mathbf{x}_2, \mathbf{y}_2) \mathrm{sinc}^2\Big(\frac{(\omega - \omega')T}{2}\Big)$$

$$+ \frac{1}{4\pi^2} \int d\mathbf{y}_1 d\mathbf{y}_2 \theta(\mathbf{y}_1) \theta(\mathbf{y}_2) \int d\omega d\omega' \hat{F}^\varepsilon(\omega) \hat{F}^\varepsilon(\omega') e^{i(\omega'+\omega)\tau + i\omega'\Delta\tau}$$

$$\times \overline{\hat{G}}(\omega, \mathbf{x}_1, \mathbf{y}_1) \hat{G}(\omega, \mathbf{x}_2, \mathbf{y}_1) \hat{G}(\omega', \mathbf{x}_1, \mathbf{y}_2) \overline{\hat{G}}(\omega', \mathbf{x}_2, \mathbf{y}_2) \mathrm{sinc}^2\Big(\frac{(\omega - \omega')T}{2}\Big). \quad (A.3)$$

Taking the limit $T \to \infty$, we see that the variance is of order $1/T$:

$$T\mathrm{Var}\big(C_T(\tau, \mathbf{x}_1, \mathbf{x}_2)\big) \stackrel{T\to\infty}{\longrightarrow}$$
$$\frac{1}{2\pi} \int d\omega \hat{F}^\varepsilon(\omega)^2 \Big| \int d\mathbf{y}_1 \theta(\mathbf{y}_1) \hat{G}(\omega, \mathbf{x}_1, \mathbf{y}_1) \overline{\hat{G}}(\omega, \mathbf{x}_2, \mathbf{y}_1) \Big|^2$$

$$+ \frac{1}{2\pi} \int d\omega \hat{F}^\varepsilon(\omega)^2 e^{2i\omega\tau} \Big| \int d\mathbf{y}_1 \theta(\mathbf{y}_1) \hat{G}(\omega, \mathbf{x}_1, \mathbf{y}_1) \overline{\hat{G}}(\omega, \mathbf{x}_2, \mathbf{y}_1) \Big|^2,$$

which quantifies the convergence rate in (4.13). Note that the first term of the asymptotic variance does not depend on τ, which means that it corresponds to fluctuations for the cross correlation around its mean $C^{(1)}$ that are stationary and extend over the whole time axis. The second term corresponds to local fluctuations. The time scale of the fluctuations of the cross correlation can be quantified from the asymptotic covariance function

$$T\mathrm{Cov}\big(C_T(\tau, \mathbf{x}_1, \mathbf{x}_2), C_T(\tau + \Delta\tau, \mathbf{x}_1, \mathbf{x}_2)\big) \stackrel{T\to\infty}{\longrightarrow}$$
$$\frac{1}{2\pi} \int d\omega \hat{F}^\varepsilon(\omega)^2 e^{i\omega\Delta\tau} \Big| \int d\mathbf{y}_1 \theta(\mathbf{y}_1) \hat{G}(\omega, \mathbf{x}_1, \mathbf{y}_1) \overline{\hat{G}}(\omega, \mathbf{x}_2, \mathbf{y}_1) \Big|^2$$

$$+ \frac{1}{2\pi} \int d\omega \hat{F}^\varepsilon(\omega)^2 e^{i\omega\Delta\tau} e^{2i\omega\tau} \Big| \int d\mathbf{y}_1 \theta(\mathbf{y}_1) \hat{G}(\omega, \mathbf{x}_1, \mathbf{y}_1) \overline{\hat{G}}(\omega, \mathbf{x}_2, \mathbf{y}_1) \Big|^2, \quad (A.4)$$

which shows that the decoherence time of the fluctuations of C_T is proportional to the decoherence time of the sources.

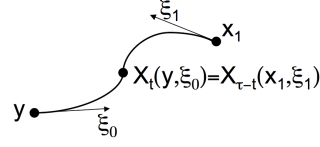FIG. B.1. *The ray connecting* **y** *and* $\mathbf{x}_1$ *is the ray starting from* **y** *with the angle vector* $\boldsymbol{\xi}_0$ *or equivalently the ray starting from* $\mathbf{x}_1$ *with the angle vector* $\boldsymbol{\xi}_1$.

Appendix B. A remark on the ray equations. The rays are solutions of Hamilton's equations [6]

$$\frac{d\mathbf{X}_t}{dt} = c_0^2(\mathbf{X}_t)\boldsymbol{\xi}_t, \qquad \mathbf{X}_0(\mathbf{x}, \boldsymbol{\xi}) = \mathbf{x},$$

$$\frac{d\boldsymbol{\xi}_t}{dt} = -\frac{1}{2}\nabla[c_0^2](\mathbf{X}_t)|\boldsymbol{\xi}_t|^2, \qquad \boldsymbol{\xi}_0(\mathbf{x}, \boldsymbol{\xi}) = \boldsymbol{\xi},$$

which derives from the Hamiltonian $H(\mathbf{x}, \boldsymbol{\xi}) = \frac{1}{2}c_0^2(\mathbf{x})|\boldsymbol{\xi}|^2$. The quantity $|\boldsymbol{\xi}_t|c_0(\mathbf{X}_t) = |\boldsymbol{\xi}|c_0(\mathbf{x}) = 1$ is constant along the ray. We assume that any pair of points in the region of interest is connected with only one ray. In other words, for any starting point **y** and any sensor **x**, there exists a unique vector $\boldsymbol{\xi}$ with norm $|\boldsymbol{\xi}|c_0(\mathbf{y}) = 1$ such that $\mathbf{X}_t(\mathbf{y}, \boldsymbol{\xi}) = \mathbf{x}$ at some time t, and then the travel time $\tau(\mathbf{x}, \mathbf{y})$ is equal to this time t.

LEMMA B.1. *1. If* $\nabla_{\mathbf{y}}\tau(\mathbf{y}, \mathbf{x}_1) = \nabla_{\mathbf{y}}\tau(\mathbf{y}, \mathbf{x}_2)$, *then* $\mathbf{x}_1$ *and* $\mathbf{x}_2$ *lie on the same side on the same ray issuing from* **y**, *and*

$$|\tau(\mathbf{y}, \mathbf{x}_1) - \tau(\mathbf{y}, \mathbf{x}_2)| = \tau(\mathbf{x}_1, \mathbf{x}_2).$$

2. If $\nabla_{\mathbf{y}}\tau(\mathbf{y}, \mathbf{x}_1) = -\nabla_{\mathbf{y}}\tau(\mathbf{y}, \mathbf{x}_2)$, *then* $\mathbf{x}_1$ *and* $\mathbf{x}_2$ *lie on the opposite sides of the same ray issuing from* **y**, *and*

$$\tau(\mathbf{y}, \mathbf{x}_1) + \tau(\mathbf{y}, \mathbf{x}_2) = \tau(\mathbf{x}_1, \mathbf{x}_2).$$

Proof. The travel time from **y** to $\mathbf{x}_1$ is associated to a unique ray. We can first look at this ray as starting from **y**, and denote by $\boldsymbol{\xi}_0$ the initial angle vector of this ray, starting from **y**. We can also look at the same ray starting from $\mathbf{x}_1$, and we denote by $\boldsymbol{\xi}_1$ the initial angle vector of this ray starting from $\mathbf{x}_1$ (see Figure B.1). We have

$$\mathbf{X}_t(\mathbf{y}, \boldsymbol{\xi}_0) = \mathbf{X}_{\tau-t}(\mathbf{x}_1, \boldsymbol{\xi}_1), \quad \boldsymbol{\xi}_t(\mathbf{y}, \boldsymbol{\xi}_0) = -\boldsymbol{\xi}_{\tau-t}(\mathbf{x}_1, \boldsymbol{\xi}_1).$$

For any time t, the angle vector is given by

$$\boldsymbol{\xi}_t(\mathbf{x}_1, \boldsymbol{\xi}_1) = \nabla_2\tau(\mathbf{x}_1, \mathbf{X}_t(\mathbf{x}_1, \boldsymbol{\xi}_1)),$$

where the gradient is taken with respect to the second point. Applying this identity at time $t = \tau(\mathbf{x}_1, \mathbf{y})$:

$$-\boldsymbol{\xi}_0 = \boldsymbol{\xi}_\tau(\mathbf{x}_1, \boldsymbol{\xi}_1) = \nabla_2\tau(\mathbf{x}_1, \mathbf{X}_\tau(\mathbf{x}_1, \boldsymbol{\xi}_1)) = \nabla_2\tau(\mathbf{x}_1, \mathbf{y}) = \nabla_{\mathbf{y}}\tau(\mathbf{y}, \mathbf{x}_1).$$

If the two points $\mathbf{x}_1$ and $\mathbf{x}_2$ are such that $\nabla_{\mathbf{y}}\tau(\mathbf{y}, \mathbf{x}_1) = \nabla_{\mathbf{y}}\tau(\mathbf{y}, \mathbf{x}_2)$, then the last equality implies that the ray connecting **y** to $\mathbf{x}_1$ and the ray connecting **y** to $\mathbf{x}_2$ must start with the same angle. This means that $\mathbf{x}_1$ and $\mathbf{x}_2$ lie on the same ray issuing from **y**. $\square$

Appendix C. The single-scattering approximation. We describe briefly the single-scattering model used in Subsection 6.2 to calculate cross correlations in the presence of reflectors, and in Section 8 to analyze coda cross correlations. We assume that the medium is characterized by a smoothly varying background velocity $c_0(\mathbf{x})$ and a set of localized scatterers around $(\mathbf{z}_j)_{j \geq 1}$. We model these scatterers as fluctuations $V(\mathbf{x})$ in the propagation speed as follows:

$$\frac{1}{c^2(\mathbf{x})} = \frac{1}{c_0^2(\mathbf{x})} + V(\mathbf{x}), \quad V(\mathbf{x}) = \sum_j \frac{1}{c_j^2} \mathbf{1}_{B_j}(\mathbf{x} - \mathbf{z}_j).$$

Here B_j are compactly supported domains. The solution of the full wave equation (4.1) can be written as a sum

$$u(t, \mathbf{x}) = u_0(t, \mathbf{x}) + u_1(t, \mathbf{x}),$$

where the direct field u_0 satisfies the wave equation (4.1) with the background velocity $c_0(\mathbf{x})$ and it is given by:

$$u_0(t, \mathbf{x}) = \int \int G_0(t - s, \mathbf{x}, \mathbf{y}) n^\varepsilon(s, \mathbf{y}) ds d\mathbf{y}, \qquad (C.1)$$

where G_0 is the Green's function of the background medium whose Fourier transform is solution of (5.1). The scattered field u_1 is given by

$$u_1(t, \mathbf{x}) = \int \int G_0(t - s, \mathbf{x}, \mathbf{y}) V(\mathbf{y}) \frac{\partial^2 u}{\partial s^2}(s, \mathbf{y}) ds d\mathbf{y}.$$

This expression is exact. The Born approximation (or single scattering approximation) consists in replacing u on the right side by the field u_0 [10]:

$$u_1(t, \mathbf{x}) \approx \int \int G_0(t - s, \mathbf{x}, \mathbf{y}) V(\mathbf{y}) \frac{\partial^2 u_0}{\partial s^2}(s, \mathbf{y}) ds d\mathbf{y}. \qquad (C.2)$$

This approximation is valid if the scattered field u_1 is small compared to the incident field u_0. We assume that the diameters of the scattering regions B_j are small compared to typical wavelength and that the velocity contrasts are such that $c_j^{-2} \mathrm{Vol}(B_j) = \varepsilon^2 \sigma_j$, with σ_j small. We can then model the scatterers by point scatterers with scattering volumes $\varepsilon^2 \sigma_j$:

$$\frac{1}{c_j^2} \mathbf{1}_{B_j}(\mathbf{x} - \mathbf{z}_j) \approx \varepsilon^2 \sigma_j \delta(\mathbf{x} - \mathbf{z}_j).$$

Substituting (C.1) into (C.2) we write the scattered field u_1 and the total field u in the form

$$u_1(t, \mathbf{x}) = \int \int G_1(t - s, \mathbf{x}, \mathbf{y}) n(s, \mathbf{y}) ds d\mathbf{y},$$

$$u(t, \mathbf{x}) = \int \int G(t - s, \mathbf{x}, \mathbf{y}) n(s, \mathbf{y}) ds d\mathbf{y},$$

where the full Green's function $G = G_0 + G_1$ and G_1 is given by

$$\hat{G}_1(\omega, \mathbf{x}, \mathbf{y}) = \varepsilon^2 \omega^2 \sum_j \sigma_j \hat{G}_0(\omega, \mathbf{x}, \mathbf{z}_j) \hat{G}_0(\omega, \mathbf{z}_j, \mathbf{y}).$$

Appendix D. Proof of Proposition 8.3. We first write the complete expression for the expectation

$$
\left\langle \widetilde{C}^{(2)}_{T',T}(\tau, \mathbf{x}_1, \mathbf{x}_2) \right\rangle = \int_{-T'}^{T'} d\tau' \frac{1}{T^2} \int_0^T \int_0^T dt dt' \int ds ds' du du' \int d\mathbf{y}_1 d\mathbf{y}_1' d\mathbf{y}_2 d\mathbf{y}_2' d\mathbf{x}_a
$$
$$
\times \chi(\mathbf{x}_a) G(s, \mathbf{x}_a, \mathbf{y}_1) G(u - \tau', \mathbf{x}_1, \mathbf{y}_2) G(s', \mathbf{x}_a, \mathbf{y}_1') G(u' - \tau' - \tau, \mathbf{x}_2, \mathbf{y}_2')
$$
$$
\times \Big(\langle n^\varepsilon(t - s, \mathbf{y}_1) n^\varepsilon(t - u, \mathbf{y}_2) n^\varepsilon(t' - s', \mathbf{y}_1') n^\varepsilon(t' - u', \mathbf{y}_2') \rangle
$$
$$
- \langle n^\varepsilon(t - s, \mathbf{y}_1) n^\varepsilon(t - u, \mathbf{y}_2) \rangle \langle n^\varepsilon(t' - s', \mathbf{y}_1') n^\varepsilon(t' - u', \mathbf{y}_2') \rangle \Big). \quad \text{(D.1)}
$$

We now use the fact that the fourth-order moments of Gaussian processes can be expanded as sums of products of second-order moments, as in the proof of Proposition 4.1. Substituting (A.2) into (D.1) we see that the limit as $T, T' \to \infty$ of $T \langle \widetilde{C}^{(2)}_{T',T} \rangle$ is equal to

$$
\widetilde{C}^{(2)}(\tau, \mathbf{x}_1, \mathbf{x}_2) = \frac{1}{2\pi} \int d\mathbf{y}_1 d\mathbf{y}_2 d\mathbf{x}_a \chi(\mathbf{x}_a) \theta(\mathbf{y}_1) \theta(\mathbf{y}_2) \int d\omega \hat{F}^\varepsilon(\omega)^2
$$
$$
\times \overline{\hat{G}}(\omega, \mathbf{x}_a, \mathbf{y}_1) \hat{G}(\omega, \mathbf{x}_1, \mathbf{y}_2) \hat{G}(\omega, \mathbf{x}_a, \mathbf{y}_1) \overline{\hat{G}}(\omega, \mathbf{x}_2, \mathbf{y}_2) e^{-i\omega\tau}.
$$

If we keep only the leading order terms in σ, then we obtain

$$
\widetilde{C}^{(2)}(\tau, \mathbf{x}_1, \mathbf{x}_2) = \frac{\varepsilon}{2\pi} \int d\mathbf{y}_1 d\mathbf{y}_2 d\mathbf{x}_a \chi(\mathbf{x}_a) \theta(\mathbf{y}_1) \theta(\mathbf{y}_2) \int d\omega \hat{F}(\omega)^2
$$
$$
\times \overline{\hat{G}_0}\Big(\frac{\omega}{\varepsilon}, \mathbf{x}_a, \mathbf{y}_1\Big) \hat{G}_0\Big(\frac{\omega}{\varepsilon}, \mathbf{x}_1, \mathbf{y}_2\Big) \hat{G}_0\Big(\frac{\omega}{\varepsilon}, \mathbf{x}_a, \mathbf{y}_1\Big) \overline{\hat{G}_0}\Big(\frac{\omega}{\varepsilon}, \mathbf{x}_2, \mathbf{y}_2\Big) e^{-i\frac{\omega}{\varepsilon}\tau}.
$$

Using the WKB approximation (5.4) of the background Green's function, we obtain:

$$
\widetilde{C}^{(2)}(\tau, \mathbf{x}_1, \mathbf{x}_2) = \frac{\varepsilon}{2\pi} \int d\mathbf{y}_1 d\mathbf{y}_2 d\mathbf{x}_a \chi(\mathbf{x}_a) \theta(\mathbf{y}_1) \theta(\mathbf{y}_2) \int d\omega \hat{F}(\omega)^2
$$
$$
\times \overline{a}(\mathbf{x}_a, \mathbf{y}_1) a(\mathbf{x}_1, \mathbf{y}_2) a(\mathbf{x}_a, \mathbf{y}_1) \overline{a}(\mathbf{x}_2, \mathbf{y}_2) e^{i\frac{\omega}{\varepsilon}\mathcal{T}(\mathbf{y}_2)},
$$

where the rapid phase is

$$
\omega \mathcal{T}(\mathbf{y}_2) = \omega [\tau(\mathbf{x}_1, \mathbf{y}_2) - \tau(\mathbf{x}_2, \mathbf{y}_2) - \tau].
$$

The analysis of the stationary points of the rapid phase is the same as in the proof of Proposition 5.1, since the rapid phase has the same expression. There are stationary points only if the points $\mathbf{y}_2$, $\mathbf{x}_1$ and $\mathbf{x}_2$ are along the same ray.

Thus, the proof of statistical stability goes along the same lines as the one of Proposition 4.1 (Appendix A), using the decomposition of the eighth-order moments of Gaussian processes as sums of products of second-order moments.

REFERENCES

[1] M. ABRAMOWITZ AND I. STEGUN, *Handbook of mathematical functions*, Dover Publications, New York, 1965.
[2] C. BARDOS, J. GARNIER, AND G. PAPANICOLAOU, *Identification of Green's functions singularities by cross correlation of noisy signals*, Inverse Problems, 24 (2008), 015011.
[3] J. BERRYMAN, *Stable iterative reconstruction algorithm for nonlinear travel time tomography*, Inverse Problems, 6 (1990), pp. 21-42.

[4] B. L. BIONDI, *3D Seismic Imaging*, no. 14 in Investigations in Geophysics, Society of Exploration Geophysics, Tulsa, 2006.

[5] D. T. BLACKSTOCK, *Fundamentals of physical acoustics*, Wiley, New York, 2000.

[6] N. BLEISTEIN, J. K. COHEN, AND J. W. STOCKWELL JR, *Mathematics of multidimensional seismic imaging, migration, and inversion*, Springer Verlag, New York, 2001.

[7] L. BORCEA, G. PAPANICOLAOU, AND C. TSOGKA, *Theory and applications of time reversal and interferometric imaging*, Inverse Problems, 19 (2003), pp. S134-S164.

[8] L. BORCEA, G. PAPANICOLAOU, AND C. TSOGKA, *Adaptive interferometric imaging in clutter and optimal illumination*, Inverse Problems, 22 (2006), pp. 1405-1436.

[9] L. BORCEA, G. PAPANICOLAOU, AND C. TSOGKA, *Optimal illumination and waveform design for imaging in random media*, J. Acoust. Soc. Am., 122 (2007), pp. 3507-3518.

[10] M. BORN AND E. WOLF, *Principles of optics*, Cambridge University Press, Cambridge, 1999.

[11] F. BRENGUIER, N. M. SHAPIRO, M. CAMPILLO, V. FERRAZZINI, Z. DUPUTEL, O. COUTANT, AND A. NERCESSIAN, *Towards forecasting volcanic eruptions using seismic noise*, Nature Geoscience, 1 (2008), pp. 126-130.

[12] F. BRENGUIER, N. M. SHAPIRO, M. CAMPILLO, A. NERCESSIAN, AND V. FERRAZZINI, *3-D surface wave tomography of the Piton de la Fournaise volcano using seismic noise correlations*, Geophys. Res. Lett., 34 (2007), L02305.

[13] M. CAMPILLO AND L. STEHLY, *Using coda waves extracted from microseisms to construct direct arrivals*, Eos Trans. AGU, 88(52) (2007), Fall Meet. Suppl., Abstract S51D-07.

[14] J. F. CLAERBOUT, *Imaging the Earth's interior*, Blackwell Scientific Publications, Palo Alto, 1985.

[15] Y. COLIN DE VERDIÈRE, *Mathematical models for passive imaging. I: general background*, arXiv:math-ph/0610043v1 (2006).

[16] Y. COLIN DE VERDIÈRE, *Mathematical models for passive imaging. II: Effective Hamiltonians associated to surface waves*, arXiv:math-ph/0610044v1 (2006).

[17] A. CURTIS, P. GERSTOFT, H. SATO, R. SNIEDER, AND K. WAPENAAR, *Seismic interferometry - turning noise into signal*, The Leading Edge, 25 (2006), pp. 1082-1092.

[18] T. L. DUVALL JR, S. M. JEFFERIES, J. W. HARVEY, AND M. A. POMERANTZ, *Time-distance helioseismology*, Nature, 362 (1993), pp. 430-432.

[19] J.-P. FOUQUE, J. GARNIER, G. PAPANICOLAOU, AND K. SØLNA, *Wave propagation and time reversal in randomly layered media*, Springer, New York, 2007.

[20] P. GOUÉDARD, L. STEHLY, F. BRENGUIER, M. CAMPILLO, Y. COLIN DE VERDIÈRE, E. LAROSE, L. MARGERIN, P. ROUX, F. J. SANCHEZ-SESMA, N. M. SHAPIRO, AND R. L. WEAVER, *Cross-correlation of random fields: mathematical approach and applications*, Geophysical Prospecting, in press (2008).

[21] E. LAROSE, L. MARGERIN, A. DERODE, B. VAN TIGGELEN, M. CAMPILLO, N. SHAPIRO, A. PAUL, L. STEHLY, AND M. TANTER, *Correlation of random wave fields: an interdisciplinary review*, Geophysics, 71 (2006), pp. SI11-SI21.

[22] O. I. LOBKIS AND R. L. WEAVER, *On the emergence of the Green's function in the correlations of a diffuse field*, J. Acoustic. Soc. Am., 110 (2001), pp. 3011-3017.

[23] A. E. MALCOLM, J. SCALES, AND B. A. VAN TIGGELEN, *Extracting the Green function from diffuse, equipartitioned waves*, Phys. Rev. E, 70 (2004), 015601.

[24] J. RICKETT AND J. CLAERBOUT, *Acoustic daylight imaging via spectral factorization: Helioseismology and reservoir monitoring*, The Leading Edge, 18 (1999), pp. 957-960.

[25] P. ROUX AND M. FINK, *Green's function estimation using secondary sources in a shallow water environment*, J. Acoust. Soc. Am., 113 (2003), pp. 1406-1416.

[26] P. ROUX, K. G. SABRA, W. A. KUPERMAN, AND A. ROUX *Ambient noise cross correlation in free space: Theoretical approach*, J. Acoust. Soc. Am., 117 (2005), pp. 79-84.

[27] L. V. RYZHIK, G. C. PAPANICOLAOU, AND J. B. KELLER, *Transport equations for elastic and other waves in random media*, Wave Motion, 24 (1996), pp. 327-370.

[28] K. G. SABRA, P. GERSTOFT, P. ROUX, AND W. KUPERMAN *Surface wave tomography from microseisms in Southern California* Geophys. Res. Lett., 32 (2005), L14311.

[29] K. G. SABRA, P. ROUX, P. GERSTOFT, W. A. KUPERMAN, M. C . FEHLER, *Extracting coherent coda arrivals from cross correlations of long period seismic waves during the Mount St Helens 2004 eruption*, Geophys. Res. Lett., 33 (2006), L06313.

[30] H. SATO AND M. FEHLER, *Wave propagation and scattering in the heterogeneous Earth*, Springer-Verlag, New York, 1998.

[31] G. T. SCHUSTER, J. YU, J. SHENG, AND J. RICKETT, *Interferometric daylight seismic imaging*, Geophysical Journal International, 157 (2004), pp. 832-852.

[32] N. M. SHAPIRO, M. CAMPILLO, L. STEHLY, AND M. H. RITZWOLLER, *High-resolution surface wave tomography from ambient noise*, Science, 307 (2005), pp. 1615-1618.

[33] R. Snieder, *Extracting the Green's function from the correlation of coda waves: A derivation based on stationary phase*, Phys. Rev. E, 69 (2004), 046610.

[34] L. Stehly, M. Campillo, and N. M. Shapiro, *A study of the seismic noise from its long-range correlation properties* Geophys. Res. Lett., 111 (2006), B10306.

[35] W. W. Symes and J. J. Carazzone, *Velocity inversion by differential semblance optimization*, Geophysics, 56 (1991), pp. 654-663.

[36] K. Wapenaar and J. Fokkema, Green's function representations for seismic interferometry, Geophysics, 71 (2006), pp. SI33-SI46.

[37] R. Weaver and O. I. Lobkis, Ultrasonics without a source: Thermal fluctuation correlations at MHz frequencies, Phys. Rev. Lett., 87 (2001), 134301.

[38] H. Yao, R. D. van der Hilst, and M. V. de Hoop, *Surface-wave array tomography in SE Tibet from ambient seismic noise and two-station analysis I. Phase velocity maps*, Geophysical Journal International, 166 (2006), pp. 732-744.